Journal of
Materials Chemistry C

PAPER

View Article Online
View Journal

Cite this: DOI: 10.1039/c6tc04530h

Facile transformation of 1-aryltriphenylenes into dibenzo[*fg*,*op*]tetracenes by intramolecular Scholl cyclodehydrogenation: synthesis, self-assembly, and charge carrier mobility of large π-extended discogens†

Ke-Qing Zhao,*[a] Min Jing,[a] Ling-Ling An,[a] Jun-Qi Du,[a] Yan-Hong Wang,[a] Ping Hu,[a] Bi-Qin Wang,[a] Hirosato Monobe,*[b] Benoît Heinrich[c] and Bertrand Donnio*[c]

Received 18th October 2016,
Accepted 13th December 2016

DOI: 10.1039/c6tc04530h

www.rsc.org/MaterialsC

The search for new organic semiconductors with enhanced charge transport properties and self-organizing abilities plays a pivotal role in the development of new applications in the emerging field of organic electronics. We have synthesized two series of discotic mesogenic materials derived from hexasubstituted triphenylene, including (i) 1-aryl-2,3,6,7,10,11-hexakis(pentyloxy)triphenylenes (14 new compounds) by a Suzuki cross-coupling reaction between the appropriate 1-bromotriphenylene precursor and various arylboronic acids and (ii) unsymmetrical facial dibenzo[*fg*,*op*]tetracene discotic molecules (11 new compounds) by an $FeCl_3$-oxidized cyclodehydrogenation reaction of the former. The mesomorphism has been investigated by polarizing optical microscopy, differential scanning microscopy, and small-angle X-ray scattering. Most aryl-substituted triphenylene derivatives exhibit a single hexagonal columnar mesophase, enantiotropic over small temperature ranges or monotropic, with this low stability being likely attributed to the free-rotating bulky side-on arene group that disrupts a perfect stacking. The corresponding more rigid and flat dibenzo[*fg*,*op*]tetracene derivatives also self-organize into a hexagonal columnar mesophase, but with a larger mesophase stability than their parents, and occurring slightly above room temperature. The UV/vis absorption and fluorescence emission spectra have been measured. Tetracenes show stronger photoluminescence than aryltriphenylene in solution, while the reversed is observed in thin films, where a strong excimer emission for one of the polar 1-aryltriphenylenes is observed. The charge carrier mobility of two representative discogens has been measured by the time-of-flight photocurrent technique. The results show that the discogen with a lateral nucleus dipole displays a hole mobility of 10^{-4} cm^2 V^{-1} s^{-1} in the mesophase, while the non-polar compound exhibits a hole mobility of 10^{-2} cm^2 V^{-1} s^{-1} in its metastable-induced ordered phase. The charge carrier mobility is discussed as a function of the supramolecular organization.

Introduction

One-dimensional columnar liquid crystalline semiconductors formed by the self-organization of discotic molecules are gaining enormous interest as attractive functional components for their potential insertion in electronic devices, including photovoltaic cells, light emitting diodes, or field effect transistors.[1,2] Discotic liquid crystals (DLCs) are usually composed of polycyclic aromatic hydrocarbons equipped with several diverging paraffinic chains. These supramolecular 1D conductive pathways, which consist of the regular stacks of disc-like π-conjugated polycyclic aromatic cores, possess both dynamical property and efficient charge carrier transporting ability along the columns, a required condition for the functioning and operation of such devices.[3,4] The efficiency of the charge transport, which determines the ultimate device performances, is however intimately connected to the molecular structure of the discogen as well as with the strength of the intermolecular interactions. This challenge thus

[a] College of Chemistry and Material Science, Sichuan Normal University, Chengdu 610066, China. E-mail: kqzhao@sicnu.edu.cn
[b] Inorganic Functional Materials Research Institute, National Institute of Advanced Industrial Science and Technology (AIST), Ikeda, Osaka 5638577, Japan. E-mail: monobe-hirosato@aist.go.jp
[c] Institut de Physique et Chimie des Matériaux de Strasbourg (IPCMS), CNRS-Université de Strasbourg (UMR 7504), 67034 Strasbourg, France. E-mail: bertrand.donnio@ipcms.unistra.fr

† Electronic supplementary information (ESI) available: Experimental techniques, POM, DSC, ^1H and ^{13}C NMR, HRMS, IR, SAXS, and HOMO–LUMO analysis. See DOI: 10.1039/c6tc04530h

motivates intense research activity in this area, essentially focused on the molecular design and synthesis of new efficient systems,[5–7] their self-organization and optoelectronic properties. It is therefore essential to explore new discogenic structures with higher charge carrier mobility[8–10] for the development of efficient, cheap and robust molecular electronic materials. The results reported in the literature seem to indicate that the carrier mobility is proportional to the size of the conjugated discogen core: the larger the aromatic core, the higher the molecule overlaps and the higher the charge carrier mobility.[11] Another approach consists in modifying the electronic properties of the core by attachment of various electro-active substituents.

An extensively studied class of DLCs is based on hexasubstituted triphenylenes,[5] but also includes for the most common ones, hexabenzocoronene[4] and phthalocyanine[6] derivatives. The great progress in modern organic synthesis methods in the last decades has made the synthesis of more structurally challenging discotic mesogens accessible, and therefore rendered the fine-tuning of their physical properties by subtle modifications possible. Transition metal catalyzed organic reactions, namely Suzuki cross-coupling[12] and Sonogashira reactions,[13] have been playing pivotal roles in the synthesis of such DLC systems.

Some classical reactions, such as the aryl oxidative cyclodehydrogenation reaction, also known as the Scholl reaction,[14,15] have been widely used in the construction of DLCs and shown high efficiency. Such an oxidative cyclodehydrogenation reaction can form multiple aromatic C–C bonds in one step to yield planar polycyclic aromatics, and has found many successful applications in the synthesis of variants of DLCs, including triphenylenes,[16] hexabenzocoronenes,[17] thiophene-fused discogens,[18] tetrabenzoanthracenes,[19] peripherally fused porphyrins,[20] triphenylene-fused triazatruxene,[21] and triphenylene-crown ether discogens.[22] Oxidative reagents, such as $FeCl_3$ in CH_2Cl_2 and/or $MeNO_2$, being low-cost and environmentally-friendly, have been widely used in aryl oxidative cyclodehydrogenation, though other chemical reagents have also been reported.[23]

As said, the Scholl reaction has greatly contributed to the synthesis of original DLCs, although, this reaction frequently competes with other mechanisms and its use still remains an important synthetic challenge. For example, the direct transformation of hexakis(4-alkoxyphenyl)benzene under the oxidative intramolecular cyclodehydrogenation conditions does not lead to the alkoxy-substituted hexa-*peri*-hexabenzocoronene (HBC)[24] but rather unexpectedly to spirocyclic dienones or indenofluorenes as main products. In some cases, semi-fused HBC intermediates could be isolated.[25] Similarly, the synthesis of hexakis(alkoxy)triphenylenes and related discogens by a direct trimerisation of 1,2-dialkoxybenzenes was found to produce monohydrolyzed coupling products,[26] or excess oxidized quinone derivatives[27] when $FeCl_3$ was used in excess. Chlorinated byproducts[15] were occasionally isolated when $FeCl_3$ was used as the oxidant. Another important challenge faced by the cyclodehydrogenation reaction is the oxidative potential dependence on the substrates,[28] as for some electron-deficient substrates, the reaction does not proceed at all. Finally, unexpected regio-isomers[29] may occasionally be produced.

In this paper, we report two novel series of discotic mesogens, derived from hexasubstituted triphenylene by the facial attachment of various phenylene, naphthalene and thiophene moieties, thereafter referred to as 1-aryltriphenylenes (**Ar-TP**) and unsymmetrical dibenzo[*fg*,*op*]tetracenes (**DBT**), which are effectively synthesized by Suzuki cross-coupling reaction and aryl oxidative cyclodehydrogenation, respectively. The mesomorphic properties of all **Ar-TP** and **DBT** compounds were investigated, and most of the derivatives exhibit hexagonal columnar mesophases, whose temperature ranges vary as a function of the molecular structure. Moreover, as the dibenzotetracene discotic core is a larger π-extended polycyclic aromatic hydrocarbon, higher charge carrier mobility than that of common triphenylene discogens may therefore be expected. In addition, the presence of electron-donating or electron-withdrawing substituents can impact both the self-organization behaviors and the charge carrier mobility. The charge carrier mobility of two **DBT** representatives was investigated by the time-of-flight photocurrent technique, and hole mobility values lying in the range of 10^{-4} to 10^{-2} $cm^2 V^{-1} s^{-1}$ were measured. The effects of dipolar functionalization on mesophase stability and charge carrier mobility are discussed.

Results and discussion

Synthetic methodology

14 new 1-aryl-2,3,6,7,10,11-hexakis(pentyloxy)triphenylenes were prepared by a Pd-catalyzed Suzuki cross-coupling reaction between the lipophilic 1-bromotriphenylene derivative and various arylboronic acids (Scheme 1). Then, in the next stage, intramolecular cyclodehydrogenation was applied to these 1-aryltriphenylenes using the $FeCl_3/H_2SO_4$ pair, which after zinc reduction and *O*-alkylation resulted in 11 new dibenzo[*fg*,*op*]tetracene derivatives (Scheme 2). In the literature, dibenzo[*fg*,*op*]tetracene is also named as dibenzo[*fg*,*op*]pyrene[27] or dibenzonaphthacene.[29,30] The structures of the final compounds were fully characterized by NMR, MS and IR (Fig. S3–S5 in ESI†).

Synthesis of 1-aryltriphenylenes (Ar-TP) by Suzuki cross-coupling. α-Bromination of hexaalkyloxytriphenylenes has allowed the synthesis of a wide variety of new π-extended arenes.[31] The key compound of this study, 1-bromo-2,3,6,7,10,11-hexakis(pentyloxy)triphenylene, **2**, was synthesized in 40% yield from 2,3,6,7,10,11-hexa(pentyloxy)triphenylene, **1**, by a modified reported method.[32] The bromination was carried out at low temperature (below 0 °C) and by slow addition of a bromine solution in CCl_4. The Suzuki cross-coupling reaction of **2** with various commercial arylboronic acids (including naphthyl and thiophene moieties) produced 1-aryl-2,3,6,7,10,11-hexa(pentyloxy)-triphenylenes **3a–n** in very high yields (79–95%, Scheme 1); the synthetic yields were hardly affected by the stereo- and electronic effects of the substrates and reagents.

Synthesis of dibenzo[*fg*,*op*]tetracenes (DBT) by intramolecular aryl oxidative cyclodehydrogenation. As mentioned above, the aryl cyclodehydrogenation faces challenges for the electro-deficient

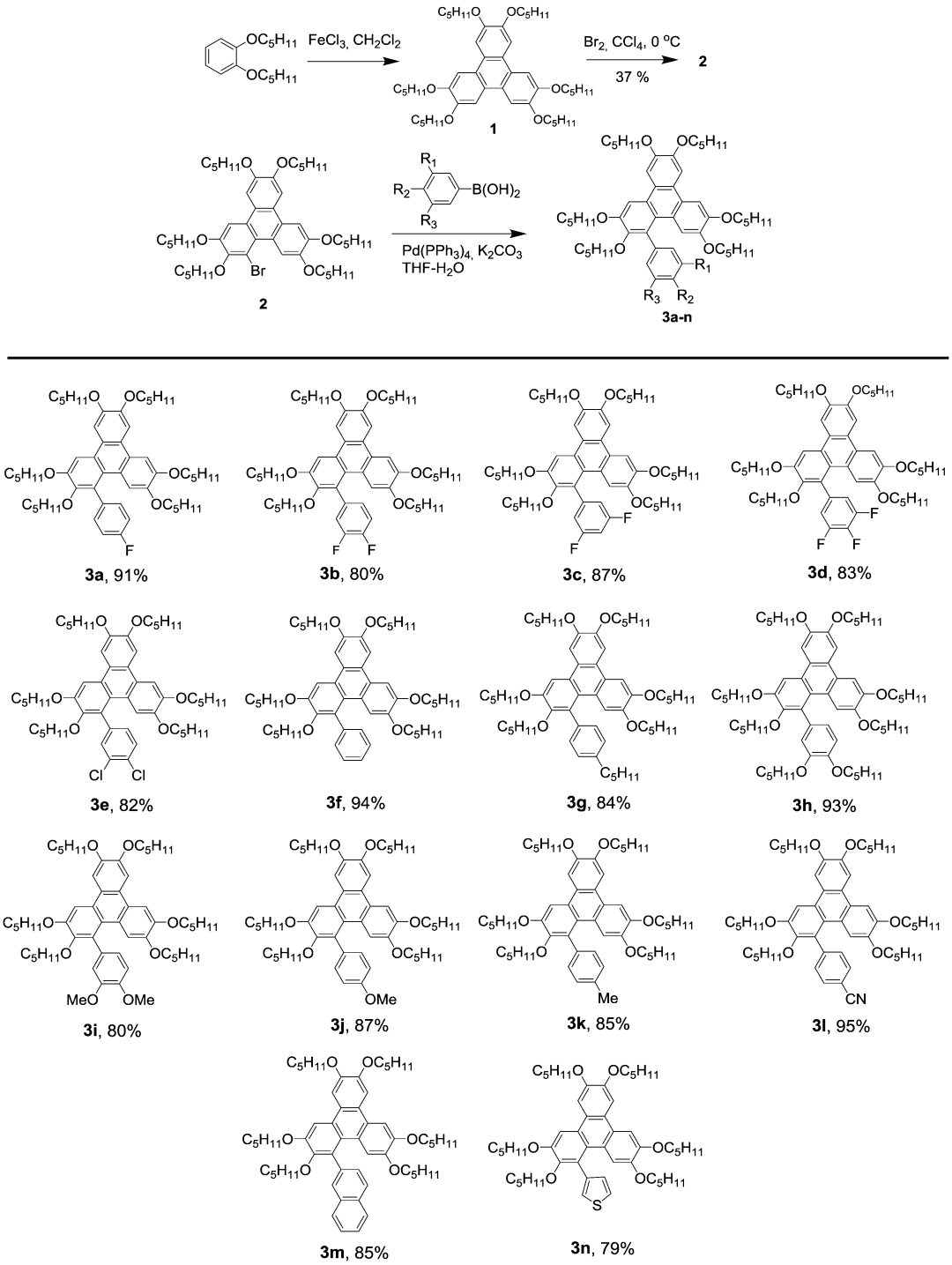

Scheme 1 Synthesis, yields and molecular structures of the 1-aryl-2,3,6,7,10,11-hexa(pentyloxy)triphenylene derivatives (**Ar-TP**, **3**).

aryl substrates.[15] The oxidative cyclodehydrogenation of 1-aryltriphenylenes **3** to dibenzo[*fg*,*op*]tetracenes **4** was optimized. For complete cyclization, excess $FeCl_3$ was used and a few drops of sulfuric acid were added. However, the dealkylation and/or formation of quinones were simultaneously observed, and both isolation and purification were tedious. These synthetic difficulties were circumvented by one-pot tandem reactions of reduction–realkylation with Zn powder/1-bromopentane/K_2CO_3. Dibenzotetracenes **4** were obtained in moderate to high yields (40–75%, Scheme 2).

It is interesting to note that 1-aryltriphenylenes with very strong electron-withdrawing substituents, such as **3d** (with three fluorine substituents) and **3l** (with a cyanide substituent), were not oxidized under the same conditions to the corresponding dibenzotetracenes, and the starting compounds were recovered from the reaction mixtures. The thiophene-substituted

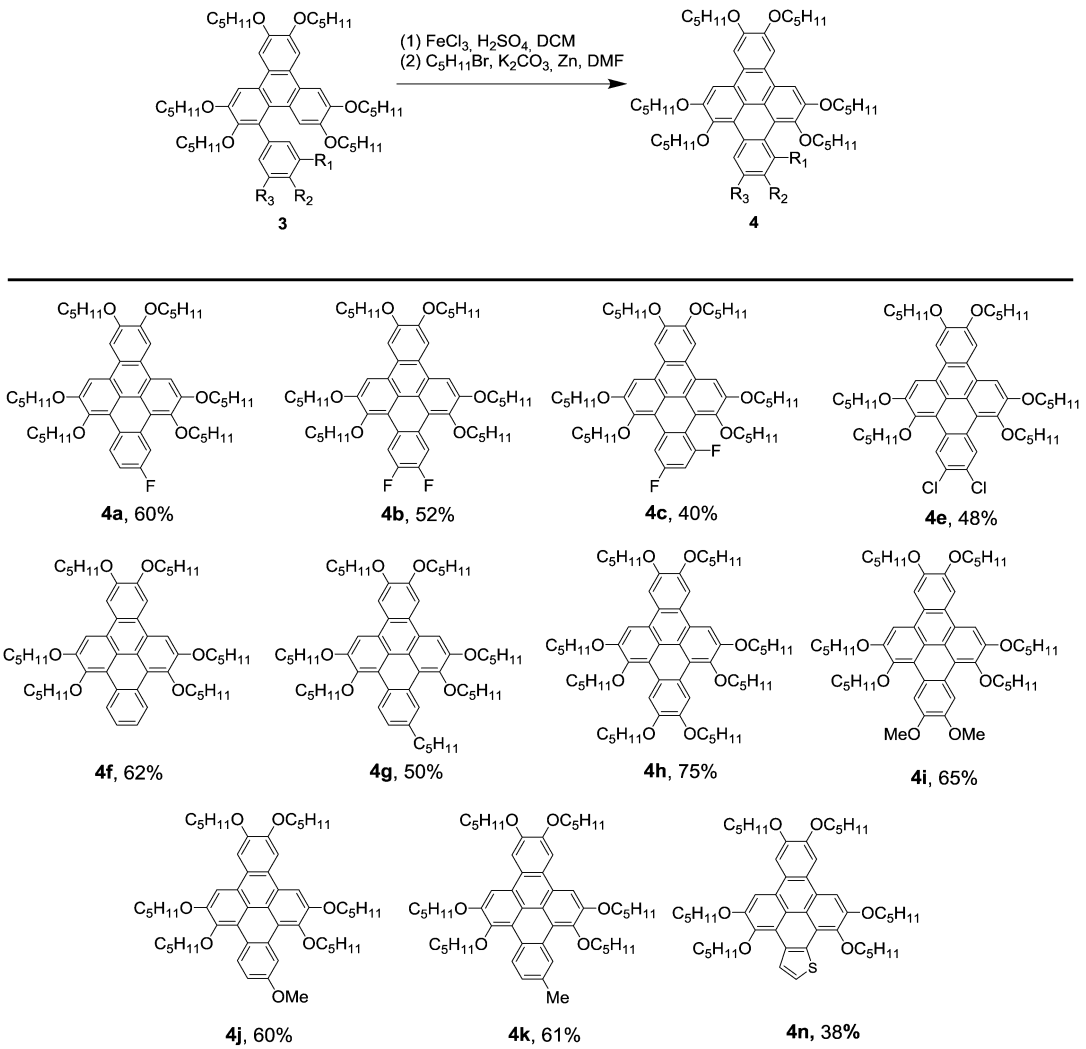

Scheme 2 Synthesis, yields and molecular structures of the dibenzo[*fg*,*op*]tetracene derivatives (**DBT**, **4**).

triphenylene **3n** was transformed to dibenzotetracene **4n**, but was unstable in the air, thus limiting the mesophase characterization by optical microscopy only. 1-Naphthalenetriphenylene **3m** was transformed, but not into the expected dibenzotetracene derivative according to the structural characterization. Finally, only the stereo less-bulky isomers were isolated in pure form (as drawn in Scheme 2).

Liquid crystalline properties

The mesomorphism of 1-aryltriphenylenes **3** and dibenzotetracenes **4** has been investigated by a combination of polarized optical microscopy (POM, Fig. 1 and Fig. S1 in ESI†), differential scanning calorimetry (Fig. S2 and Table S1 in ESI†), and small-angle X-ray scattering (SAXS, Fig. 4, Fig. S6 and Table S2 in ESI†). As displayed in Fig. 1, most compounds of both series **3** and **4** show fluid, birefringent, fan-shaped optical textures with large homeotropic domains characteristic of the formation of a columnar hexagonal mesophase (Col_{hex}).

Mesomorphism of 1-aryltriphenylenes, 3. Hexakis(pentyloxy)triphenylene **1** is an archetypal columnar liquid crystal, with a broad

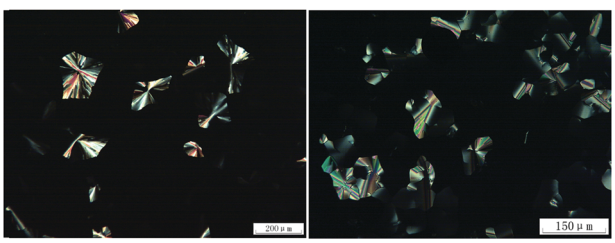

Fig. 1 Typical optical textures of two representatives of the **Ar-TP** and **DBT** series: **3k** at 60 °C; **4k** at 65 °C, on cooling from the isotropic liquid, respectively (scale bars are 200 and 150 μm, respectively).

enantiotropic hexagonal columnar (Col_{hex}) range from 65 to 121 °C.[33] In the Col_{hex} phase, the disc-like cores stack face-to-face into columns, disposed at the nodes of a two-dimensional lattice and nanosegregated from peripheral molten chains merging to a continuum. Although of the same chemical nature, the appending phenyl unit of the aryltriphenylene cores is a typical segment of rod-like mesogens,[34] because of the rapid rotation around the sigma bond axis conferring an average

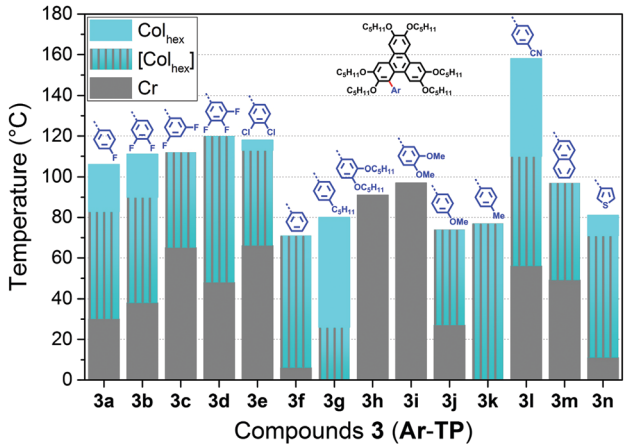

Fig. 2 Phase diagram of compounds of series **3**. Cr: crystalline phase; Col$_{hex}$: enantiotropic hexagonal columnar phase; [Col$_{hex}$]: monotropic hexagonal columnar phase.

cylindrical shape.[35] The rigid linking between two mesogenic units self-associating in a different way is inevitably detrimental to mesomorphism, and the bare phenyl derivative **3f** only shows a monotropic Col$_{hex}$ phase with *ca.* 80 °C drop of the transition to the isotropic liquid (the isotropization) with respect to pure discotic **1** (Fig. 2). Conversely, the mesophase is still enantiotropic and the drop is limited to 40 °C in **3n**, due to the propensity for face-to-face stacking of its thiophenyl substituent.[36] In contrast, the increase of the substituent size from phenyl to naphthyl (**3m**) does not promote the Col$_{hex}$ phase, which is monotropic, with just upward shifts of melting and isotropization temperatures.

Beyond the impeded stacking, the expansion of the core by bare substituents introduces an imbalance with the number of chains, beforehand optimal in unsubstituted **1**.[37] A single pentyl tail on phenyl cancels this lack of chains and explains that the isotropization temperature of **3g** is 40 °C above that of **3f**. Intermediate transition temperatures are logically found with a single methyl or methoxy group (**3k** and **3j**), since the insertion of such short tails between longer tails is less beneficial for a cohesive lateral packing. The space requirement of two chains clearly exceeds the void created by the core expansion as shown by the total disappearance of the mesomorphism for derivatives **3h** and **3i**.

The use of phenyl substituents bearing polar groups could induce more cohesive structures through the dipolar interactions within and between the columns, and also through the repelling of the tails and the denser periphery. In that line, the isotropization temperatures of derivatives with fluoro or chloro groups in the *meta* and *para* positions of the protruding phenyl ring (**3a–e**) were found to extend far beyond that of **3f** and to result in enantiotropic Col$_{hex}$ ranges when at least one *meta* position stays unsubstituted (**3a**, **b**, and **e**). The isotropization temperature shift is not so large when both *meta* positions are substituted (**3c** and **d**), while the melting temperature increases quite regularly with the number of halogens. The effect on the columnar range is therefore canceled in this particular case, presumably in relation with the 120° angle between *meta* positions, as such an angle is logically unfavorable for directed intermolecular interactions. In liquid crystalline mesophases, the cyano group shows the highest potential for dipolar association,[38] and the isotropization temperature of the cyano derivative **3l** consistently lies 50 °C above that of the fluoro analogue **3a**, for a 25 °C enlargement of the enantiotropic range (Fig. 2) and the largest mesomorphic range.

Mesomorphism of the functionalized dibenzo[*fg*,*op*]-tetracenes, 4. After cyclodehydrogenation, the substituted phenyl and triphenylene segments fuse to yield a unique large-size conjugated discotic mesogen. The self-organization process is therefore deeply modified from bare phenyl derivative **3f** to **4f**, in consistency with a substantial increase of the isotropization temperature and with the appearance of an enantiotropic Col$_{hex}$ range (Fig. 3). In contrast, the isotropization temperature is already relatively high in **3n** and stays roughly the same in **4n**, in accordance with the expected π-stacking of the entire core before and after cyclodehydrogenation.

The variation of the number and size of chains (**4g**, **h**, **j**, and **k**) proved a maximum extension of the mesomorphous range for the derivative with eight pentyl chains (**4h**). In contrast, the presence of two methoxy groups is detrimental to mesomorphism for **4i**. The influence of polar groups follows the same trend as that of precursors: high isotropization temperatures for the derivatives with fluoro or chloro groups in the *para* and *meta* positions (**4a**, **b**, and **e**), and the absence of mesomorphism for the derivative with fluoro groups in both *meta* positions (**4c**) (Fig. 3).

Characterization of the mesophases by small angle X-ray scattering (SAXS). SAXS patterns could be recorded for four derivatives of the aryltriphenylene series, namely **3f** and **3k** (with phenyl and methylphenyl substituents) in the monotropic Col$_{hex}$ phase, and **3b** and **3l** (the difluorophenyl and cyano derivatives) in their enantiotropic Col$_{hex}$ range (Fig. 4, Fig. S6 and Table S2 in ESI†). The signature of the nanosegregated structure at small angles proves in both cases a hexagonal lattice with one single column, with an intense first-order reflection (10) around 17 Å and a series of weaker, higher-order reflections, according to spacing ratios $\sqrt{3}$, 2, $\sqrt{7}$ and indexations (11), (20) and (21), respectively.

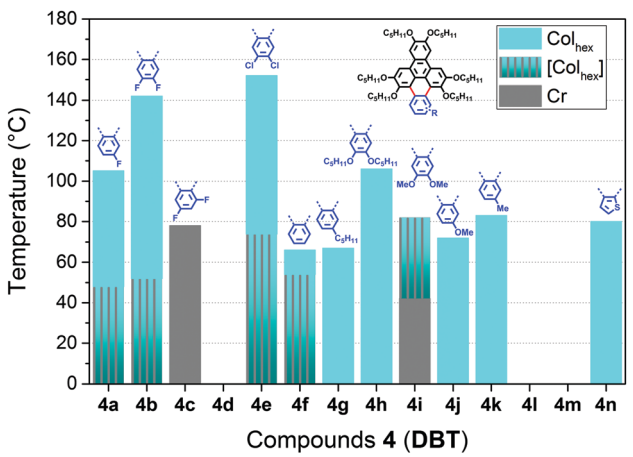

Fig. 3 Phase diagram of compounds of series **4**.

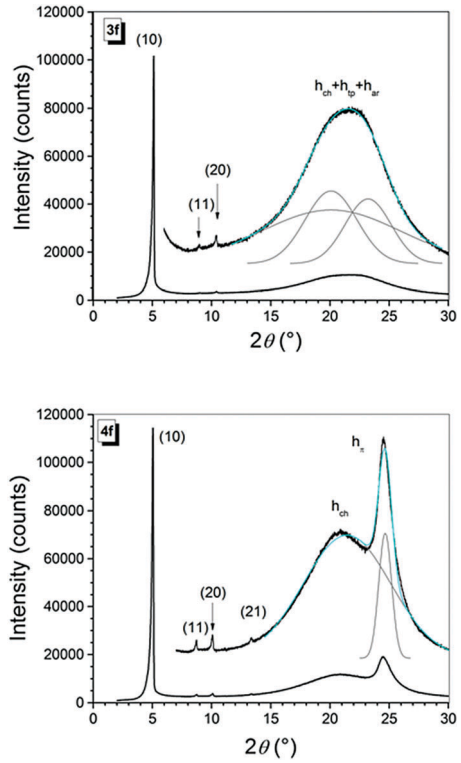

Fig. 4 Representative SAXS patterns of one derivative of each series: **3f** and **4f** at 25 °C (h_{ar}, h_{ch}, h_{tp} and h_{π} are defined in the text).

The packing features inside domains can be taken from the wide-angle region, in which the absence of the characteristic semi-diffuse scattering maximum from π-stacked triphenylene h_{π} (usually located around 3.5 Å)[33] is immediately noticed. This peculiarity is obviously related to the rigid bond with the phenyl substituent, which as a sub-unit of calamitic mesogens is associated with larger lateral distances (typically 4.5–4.8 Å, h_{ar}).[39]

Triphenylene rings therefore accommodate this mismatch between natural distances through their piling in a very irregular way (h_{tp}), which explains the disappearance of the characteristic h_{π} signal. Instead, the entire rigidly linked mesogens give rise to a unique broad scattering (h_{ar} + h_{tp}), whose ill-defined maximum is located at intermediate distances and overlaps with the contribution from the molten aliphatic continuum, h_{ch}. Consistently, the molecular slice thicknesses h_{mol} (=V_{mol}/S_{col}, where V_{mol} is the calculated molecular volume from reference density data and S_{col}, the lattice area) are also intermediate between both natural distances (h_{mol} ≈ 3.9 Å for **3f** and **3k** and 4.2–4.3 for **3b** and **3l**, Table 1), while a coincidence between h_{mol} and h_{π} (≈3.5 Å) was found for the neat triphenylene compound **1**.[33]

SAXS patterns were recorded for six derivatives of the dibenzotetracene series, namely the unsubstituted derivative **4f**, compared on the one hand to derivatives with one methyloxy group (**4j**), one methyl group (**4k**) and two pentyloxy chains (**4h**), following the order of isotropization temperatures, and on the other hand, to derivatives with fluoro or chloro groups in the *meta* and *para* positions (**4b** and **4e**), for which the Col_{hex} phase is maintained at high temperature (Fig. 3).

Table 1 SAXS results of the representative 1-aryltriphenylenes and dibenzo[*fg*,*op*]tetracenes[a]

Compounds	Phase and parameters
3b	Col_{hex}, a = 19.36 Å, S_{col} = 324.7 Å^2 V_{mol} = 1360 Å^3, h_{mol} = 4.2 Å
3k	Col_{hex}, a = 19.79 Å, S_{col} = 339.4 Å^2 V_{mol} = 1336 Å^3, h_{mol} = 3.9 Å
3l	Col_{hex}, a = 19.54 Å, S_{col} = 331.0 Å^2 V_{mol} = 1430 Å^3, h_{mol} = 4.3 Å
3f	Col_{hex}, a = 19.64 Å, S_{col} = 334.1 Å^2 V_{mol} = 1309 Å^3, h_{mol} = 3.9 Å
4b	Col_{hex}, a = 20.18 Å, S_{col} = 352.5 Å^2 V_{mol} = 1319 Å^3, h_{mol} = 3.74 Å
4e	Col_{hex}, a = 20.01 Å, S_{col} = 346.8 Å^2 V_{mol} = 1339 Å^3, h_{mol} = 3.86 Å
4f	Col_{hex}, a = 20.23 Å, S_{col} = 354.4 Å^2 V_{mol} = 1298 Å^3, h_{mol} = 3.66 Å
4j	Col_{hex}, a = 20.06 Å, S_{col} = 348.8 Å^2 V_{mol} = 1331 Å^3, h_{mol} = 3.82 Å
4k	Col_{hex}, a = 20.04 Å, S_{col} = 348.0 Å^2 V_{mol} = 1325 Å^3, h_{mol} = 3.81 Å
4h	Col_{hex}, a = 21.94 Å, S_{col} = 416.8 Å^2 V_{mol} = 1585 Å^3, h_{mol} = 3.80 Å

[a] $a = 2 \times \sum[d_{hk}(h^2 + k^2 + hk)^{1/2}(N_{hk}\sqrt{3})^{-1}]$, where N_{hk} is the number of hk reflections for the Col_{hex} phase; V_{mol} is the molecular volume, S_{col} is the lattice area and $h_{mol} = V_{mol}/S_{col}$ is the molecular thickness (see Table S2 in the ESI).

The SAXS patterns (Fig. 4) turned out to be very similar for all compounds, with the same sharp small-angle reflections series (10), (11), (20) and (21) from a hexagonal lattice with one single column, and with nearly identical wide-angle regions. In particular, the semi-diffuse h_{π} scattering signal re-appears next to broad scattering h_{ch}, which confirms the transformation of the core into a unique π-stacking mesogen. The comparison of h_{mol} (**4f**: ≈3.6 Å; **4j**, **k**, **h**, **b**, and **e**: ≈3.8 Å, Table 1) and h_{π} (≈3.6 Å) ends up with minor differences, compatible with the absence of tilting or small tilt angles of cores within the columns.[40] The molecular packing in the Col_{hex} phase is therefore similar to that of **1**, except that the aspect ratio is close to 1.2 for the new dibenzotetracene core, which implies that the mesogen orientations vary inside columnar domains to preserve the hexagonal symmetry.

Interestingly, it is worth mentioning that some other structurally related **DBT** DLCs (Fig. S9 in ESI†) have already been reported in the literature.[27,29,30] The symmetrical hexa(pentyloxy)-**DBT** displays an ordered Col_{hex} mesophase between 121 and 223 °C (with a stacking distance of 3.55 Å at 150 °C),[30] that is at much higher temperatures than compounds **4**, and particularly with respect to its structural isomer **4f**, highlighting the importance of the substituent positions and nature. Similarly, octakis(pentyloxy)-**DBT**, a symmetrical isomer of **4h**, shows in contrast a lower clearing temperature of 94 °C, with a slightly larger aryl core–core distance value of 3.81 Å (at 67 °C).[27] This result can be explained by the stereo perturbation of the two extra alkoxy peripheral chains, which weaken the π–π interactions and the discotic staking with respect to compounds with lesser chains. Mesomorphic properties are apparently strongly dependent on the chains anchoring positions too (as compared with **4h**). Most recently, a series of tetra-substituted dibenzo[*fg*,*op*]tetracenes has been synthesized and reported to possess smectic A (SmA) and C

(SmC) phases, as well as the hexatic-B phase.[30] It is obvious that the semiconducting properties of 1-dimensional columnar and 2-dimensional smectic mesophases based on this polycyclic aromatic core are highly worth further studying. This study indeed emphasizes once more the importance of molecular engineering of mesogens to tune the transport properties of liquid crystalline semiconductors. All **DBT 4** synthesized here, exhibiting a Col_{hex} mesophase at room temperature and low phase transition temperatures, are advantageous for thermal annealing for homeotropic alignment of the samples and self-healing the defects formed during self-assembly, and offer novel perspectives for the fabrication of high performance active layers for organic optoelectronic devices.

Charge transport properties investigated by the time-of-flight (TOF) photocurrent technique

The charge carrier mobility is the most important parameter for organic semiconductors as it essentially determines their future performance in devices. For liquid crystalline semiconductors, main factors such as the mesogenic core- and its electronic properties, as well as the mesomorphic supramolecular structure, have a direct and important effect on the charge transport properties. We have investigated the charge carrier mobility of two representative discogens, **4b** and **4i**, by the time-of-flight (TOF) photocurrent technique, and the results are shown in Fig. 5 and 6.

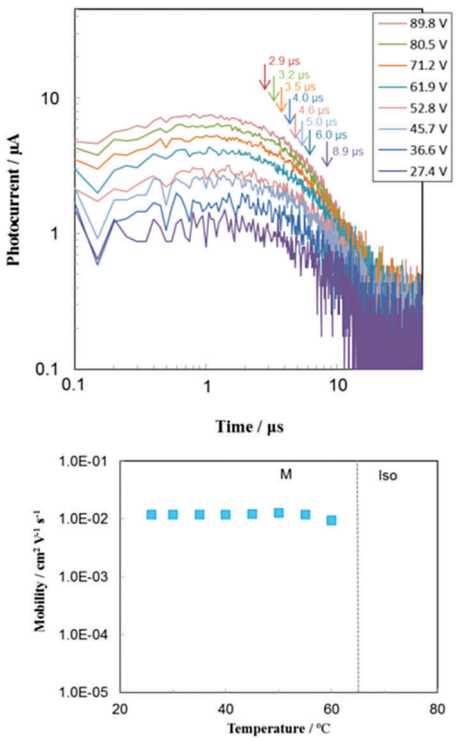

Fig. 5 Charge carrier mobility of **4i** (measured by the time-of-flight photocurrent technique, cell thickness 16.8 µm). Top: Bias-dependent photocurrent decay curves at 55 °C with the drift times labeled on the curves (hole, log–log plot). Bottom: Temperature dependence of charge carrier mobility on cooling (hole).

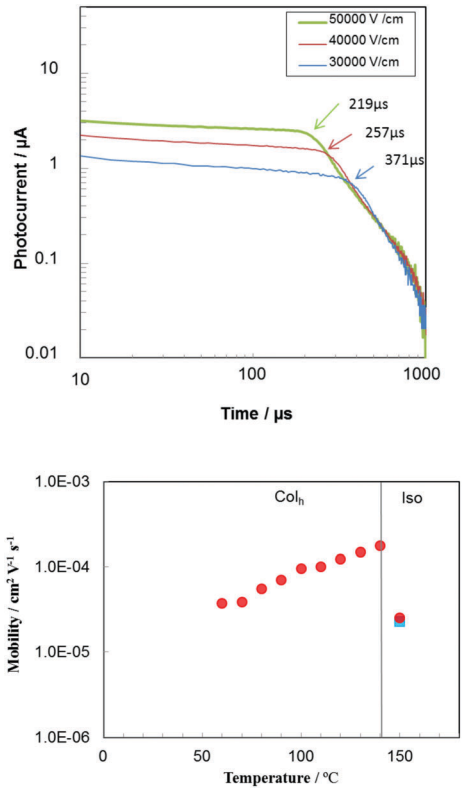

Fig. 6 Charge carrier (hole) mobility of **4b** (measured by time-of-flight photocurrent technique, cell thickness 16.2 µm). Top: Electric field dependency of positive photocurrent curves (log–log plot) at 130 °C; bottom: temperature dependence of charge carrier mobility for positive (circle) and negative (square) charge carrier transports on cooling.

First, the liquid crystalline homeotropic aligned sample **4i** in an ITO cell was irradiated with an N_2 laser (337 nm) and the transient photocurrent decay curves were non-dispersive for positive charges (holes) at various electric fields (Fig. 5). The measured positive charge mobility value, μ_{hole}, is of the order of 10^{-2} cm^2 V^{-1} s^{-1}. Considering the distance of 16.8 µm for the charge carrier hopped along the supramolecular discotic columns, this TOF mobility value is quite high, and one to two orders of magnitude higher than the transport value of 10^{-4}–10^{-3} cm^2 V^{-1} s^{-1} exhibited by triphenylene discogens.[41] More interestingly, the hole mobility was temperature- and electric-field-independent. However, the negative charge (electron) photocurrent was not detected for **4i**, feasibly due to the higher sensitivity of the electron to oxygen, moisture, and organic impurity. **4i**, as an electron-rich discogen, favors hole transport and is thus a p-type discotic semiconductor. Furthermore, as this discogen has a low clearing temperature and a mesophase temperature range covering the operational-significant room temperature, it posits as a very useful candidate for electronic device applications.

The charge mobility measurement of one dipolar homolog, **4b**, reveals both positive and negative charge transport abilities, and the photocurrent decay curves are non-dispersive (Fig. 6). Its hole charge mobility value reaches 2×10^{-4} cm^2 V^{-1} s^{-1} in the mesophase. Both positive negative charge mobilities are

1.2×10^{-5} cm^2 V^{-1} s^{-1} in the isotropic phase indicating the existence of ionic charge transport. The photocurrent decay curves are non-dispersive and the mobility value is slightly temperature dependent.

These two discogens possess the same aromatic core, and both discogens are hole transporters. However, their carrier mobility values differ by two orders of magnitude. **4b** has a strong dipolar nucleus, with two fluoro-substituents on one side pulling electrons and six pentyloxy groups on the other side of the molecule pushing electrons. Therefore, in the supramolecular discotic columns, discs **4b** likely stack on top with an antiparallel orientation. Thus, the charged carriers (holes) hope along these electronically disordered columns at a low rate. On the contrary, **4i** is non-polar, with no preferential orientation, and the discotic columns as charged-carrier pathways are electronically neutral, therefore promoting a much faster hole mobility rate.

Related results have been reported in the literature. For instance, the charge transport property of a few dipolar discotic liquid crystalline systems, *e.g.* triphenylene discogens substituted with nitro-[42] or ester[43] groups, and a discotic quinone,[44] was found to decrease as well as be temperature- and electric field-dependent. The electronic and energetic disorder in the columns was suggested to be responsible for this decreased charge transport value. However, 1,4-difluoro-2,3,6,7,10,11-hexa(pentyloxy)triphenylene[45] showed enhanced mobility with a slight temperature and electric field-dependence. The authors argued that the dipole benefited the ordered staking of the discogens into the columns and therefore improved the charge transport. So, dipoles seem to have two opposite effects: one enhancing the discotic columnar superstructures, and the other causing electronically disordered antiparallel orientation of the molecules in the discotic columns. Which of these two opposite effects dominates is still a puzzle and might be discotic system dependent, therefore more explorations are needed.

In our case, the difference in the thermal stability of mesophases may offer an alternative explanation. A careful investigation of the thermal behavior reveals that the mesophase of **4i** is indeed metastable, whilst it is enantiotropic for **4b**, with this enhanced stability being associated with the presence of the lateral fluoro dipoles. For **4i**, crystallization begins once in the (monotropic) mesophase, with no temperature change, with this tendency being amplified in the thin film morphology. A columnar structure-orientated crystallization process would therefore contribute to this difference, likely by favoring a perfect stacking of the mesogens into columns while reducing the formation of grain boundaries during this gradual mesophase-to-crystalline phase transformation and the consequent rigidification, therefore improving the charge transport properties within columns, with respect to **4b** which is still fluid and subjected to perturbations.

Photophysical properties of 1-aryltriphenylene and dibenzotetracene derivatives – UV/vis absorption and fluorescent emission

The photophysical properties of 1-aryltriphenylenes **3** and dibenzotetracenes **4** are interesting as their π-conjugated systems varied from triphenylene. The UV/vis absorption in solution and fluorescence emission in both solution and solid film are shown in Fig. 7 and the results are summarized Table 2.

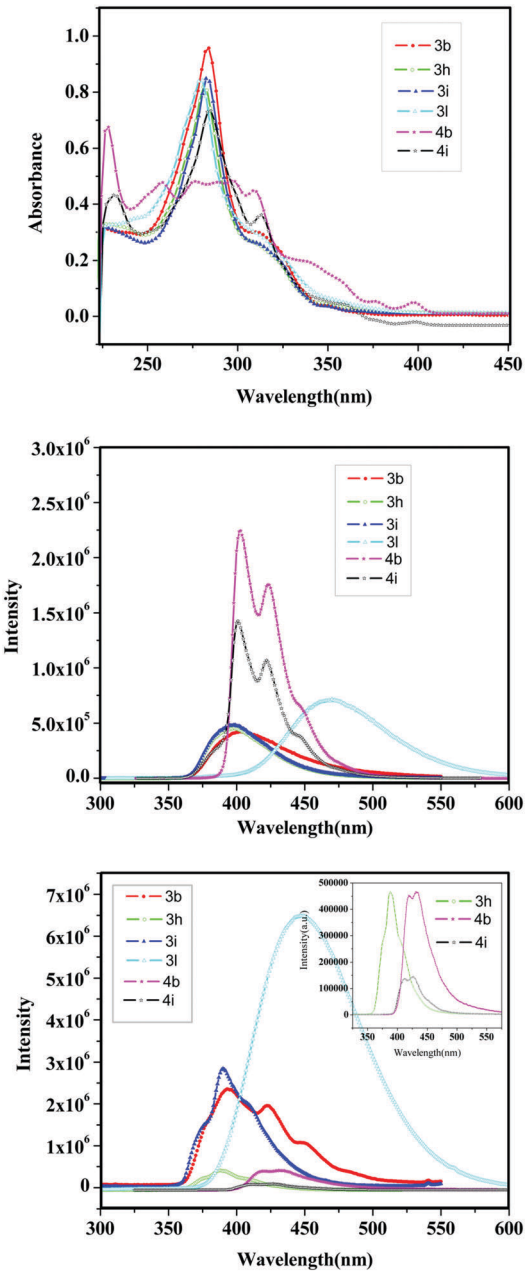

Fig. 7 UV/vis (top) and fluorescence (middle in solution, bottom in film) spectra of 1-aryltriphenylene and dibenzotetracene derivatives (in CH_2Cl_2, 1.0×10^{-5} M).

The absorption spectra of 1-aryltriphenylenes (**3b**, **h**, and **i**) and tetracene (**4i**) display the strongest absorption at $\lambda = 284$ nm that originates from the absorption of the triphenylene core (Fig. 7).[46,47] **4b** shows a strong broad absorption band between 250–310 nm and several weak absorptions between 310 and 400 nm. All discogens exhibit molar absorption coefficients in the range of 5–10 $\times$ 10^4 L mol^{-1} cm^{-1}.

In solution, the photoluminescence of tetracenes (**4b** and **4i**) is stronger than that of 1-aryltriphenylenes **3** (Fig. 7), possibly

Table 2 Summary of the UV/vis absorption and fluorescence spectroscopic properties of discogens in solutions and films

	Solution			
	λ_{abs} [nm]	ε [L mol^{-1} cm^{-1}]	λ_{em} [nm] QY (%)	Film λ_{em} [nm]
3b	284	1×10^5	403 (1.59)	255, 422
3h	284	8×10^4	398 (1.32)	389
3i	283	8×10^4	398 (0.98)	390
3l	279	8×10^4	472 (2.33)	447
4b	228	7×10^4	403 (3.19)	420
	258	5×10^4	433	
	297	5×10^4		
	310	4×10^4		
	398	4×10^3		
4i	232	5×10^4	401 (2.65)	413
	283	8×10^4	422	427
	312	4×10^4		

For the emission measurement, the samples were excited with λ_{ex} = 284 nm, expect for **4b**, which was excited with 297 nm. QY: quantum yield efficiency.

due to the later exhibiting partial fluorescence quenching caused by free rotation of the sigma bond between phenyl and triphenylene core. It is noted that **3l** shows a broad emission band with a peak at 472 nm, larger than all discogens studied here, and likely corresponds to the excimer emission of **3l**, due to the natural tendency for antiparallel dimerization of the polar molecule, as shown above.

On the contrary, the fluorescence emission of **3** in film is stronger than that of **4** (Fig. 7), as this time the π–π stacking of tetracenes **4** results in partial emission quenching. Obviously **3l** shows the strongest green light emission with a peak centered at 447 nm, blue-shifted by 25 nm from the emission in solution. Thus, as expected tetracenes **4** display higher quantum yield efficiency than 1-aryltriphenylene **3** in solution, but this is reverted in films. In addition, it was found that polar compounds show higher QY than non-polar compounds (Table 2). The strong light emitting property of 1-aryltriphenylenes **3** as well as their self-organization into a columnar mesophase implies their potential applications in sensors for explosive chemicals (nitro-substituted arenes such as TNT) and light emitting and electronic charge carrier materials in OLEDs.

Conclusions

Fourteen members of 1-aryl-2,3,6,7,10,11-hexakis(pentyloxy)-triphenylenes have been synthesized in high yields by the Suzuki cross-coupling reaction of 1-bromo-2,3,6,7,10,11-hexakis-(pentyloxy)triphenylene with arylboronic acids. Quite surprisingly, most aryltriphenylenes are still capable of self-organizing into a columnar hexagonal mesophase, but display lower isotropization temperatures than the parent compound 2,3,6,7,10,11-hexakis(pentyloxy)triphenylene. The only exception is the 4-cyanophenyl-substituted triphenylene, which shows the highest isotropization temperature.

The intramolecular oxidative cyclodehydrogenation by $FeCl_3$ oxidation, followed by realkylation have successfully yielded eleven novel dibenzo[*fg*,*op*]tetracene discogens. These unsymmetrical **DBT** discogens display broad mesophase ranges covering the operationally-significant room temperature. The isotropization temperatures of these mesogens are dependent on the electronic properties of the substituents: electron-withdrawing groups increase the isotropization temperature, while electron-donating groups decrease the T_i. The strong lateral nucleus dipole feasibly induces the antiparallel alignment of discogens into in the columns and therefore stabilizes the columnar mesophase.

These 1-aryltriphenylenes and dibenzotetracenes display UV absorption similar to triphenylene discogens and possess strong fluorescence emission of blue or green light in both solution and thin film. Unexpectedly the film of **3l** exhibits strong excimer emission of green light. Importantly, the semiconducting properties of two representative dibenzotetracene discogens, **4i** and **4b**, have been investigated by the time-of-flight photocurrent technique, they display hole mobility rates of 10^{-2} cm^2 V^{-1} s^{-1} and 10^{-4} cm^2 V^{-1} s^{-1}, respectively. The introduced lateral molecular dipole in **4b** and the resultant antiparallel molecular orientation promote strong stability of the Col_{hex} mesophase with respect to **4i**, but the charge carrier transport, due to the energetic and electronic disorder within the supramolecular columns, is disfavoured. In contrast, the low thermodynamic stability of the phase of **4b** is actually very useful as it permits the pre-organization of the molecules into columns whilst preserving the columnar structure during crystallization.

In this study, we emphasize once more the importance of the molecular design to tune the transport properties of liquid crystalline semiconductors. The facile synthetic method described here to generate a wide range of substituted dibenzotetracene discogens offers novel perspectives for the fabrication of high performance active layers for organic optoelectronic devices.

Experimental section

General instruments and compounds characterization are reported in the ESI.† 1,2-Di(pentyloxy)benzene[16b] and 2,3,6,7,10,11-hexakis-(pentyloxy)triphenylene, **1** were prepared according to a reported method.[16b]

2: 1-bromo-2,3,6,7,10,11-hexakis(pentyloxy)triphenylene, **2**, was synthesized by a modified reported method.[32a] To a stirred solution of 2,3,6,7,10,11-hexa(pentyloxy)triphenylene (1, 20 g, 26.9 mmol) in CCl_4 (150 mL) cooled to −10 °C, Br_2 (4.4 g, 27.5 mmol) in CCl_4 (20 mL) was added slowly, and the mixture was stirred below 0 °C for 10 h. Then, a sodium metabisulfite solution (20%) was added. The organic extracts were combined, washed with brine, dried over $MgSO_4$, and concentrated *in vacuo*. The residue was purified by column chromatography on silica gel, eluted with light petroleum ether/CH_2Cl_2 (3 : 2, v/v), and crystallized from ethanol to yield a white solid (8.2 g, 37%). ^{1}H NMR ($CDCl_3$, TMS, 400 MHz) δ: 9.00 (s, 1H, 1ArH), 7.81 (s, 1H, 1ArH), 7.77 (s, 3H, 3ArH), 4.23 (t, J = 6.4 Hz, 10H, 5ArOCH_2), 4.11 (t, J = 6.8 Hz, 2H, 1ArOCH_2), 1.94 (m, 12H, 6CH_2), 1.55 (m, 12H, 6CH_2), 1.45 (m, 12H, 6CH_2), 0.98 (t, J = 7.2 Hz, 18H, 6CH_3).

3a: under argon atmosphere, to a flask containing **2** (500 mg, 0.61 mmol), (4-fluorophenyl)boronic acid (169.81 mg, 1.21 mmol),

anhydrous K_2CO_3 powder (1.26 g, 9.13 mmol), $Pd(PPh_3)_4$ (69.78 mg, 0.061 mmol), deoxygenated THF (12 mL) and distilled water (3 mL) were added. The mixture was stirred at 80 °C for 18 h. Then, the mixture was cooled, poured into 2 N HCl aqueous solution, and extracted with CH_2Cl_2. The organics were dried over $MgSO_4$, filtered, and concentrated in vacuum. The residue was purified by silica gel column chromatography, eluted with light petroleum/CH_2Cl_2 (3 : 2, v/v), and crystallized from ethanol to give a white solid, **3a** (463.4 mg, 91%). ^{1}H NMR ($CDCl_3$, TMS, 400 MHz) δ: 7.87 (d, J = 8.0 Hz, 2H, 2ArH), 7.78 (s, 1H, 1ArH), 7.72 (s, 1H, 1ArH), 7.39 (d, J = 8.4 Hz, 2H, 2ArH), 7.13 (s, 3H, 3ArH), 4.27 (t, J = 6.4 Hz, 8H, 4ArOCH$_2$), 3.60 (t, J = 6.4 Hz, 2H, 1ArOCH$_2$), 3.25 (t, J = 6.4 Hz, 2H, 1ArOCH$_2$), 1.87–1.97 (m, 8H, 4CH$_2$), 1.66–1.69 (m, 2H, 1CH$_2$), 1.52–1.59 (m, 6H, 3CH$_2$), 1.36–1.50 (m, 16H, 8CH$_2$), 1.06–1.17 (m, 4H, 2CH$_2$), 0.95 (t, J = 7.2 Hz, 15H, 5CH$_3$), 0.83 (t, J = 7.2 Hz, 3H, 1CH$_3$).

All the other 1-aryl-triphenylene derivatives, **3b–n**, were synthesized and purified accordingly.

3b: **2** (130 mg, 0.16 mmol), (3,4-difluorophenyl)boronic acid (49.83 mg, 0.32 mmol). **3b**: 108.18 mg, 80%. ^{1}H NMR ($CDCl_3$, TMS, 400 MHz) δ: 8.17 (s, 1H, 1ArH), 8.13 (s, 1H, 1 ArH), 8.05 (s, 1H, 1ArH), 7.99 (s, 1H, 1ArH), 7.52 (d, J = 6.0 Hz, 1H, 1ArH), 7.48 (d, J = 6.4 Hz, 1H, 1ArH), 7.36 (s, 2H, 2ArH), 4.51 (t, J = 6.4 Hz, 6H, 3ArOCH$_2$), 4.43 (t, J = 6.4 Hz, 2H, 1ArOCH$_2$), 3.88 (t, J = 6.4 Hz, 2H, 1ArOCH$_2$), 3.55 (t, J = 6.4 Hz, 2H, 1ArOCH$_2$), 2.21–2.24 (m, 8H, 4CH$_2$), 1.96–1.99 (m, 2H, 1CH$_2$), 1.63–1.84 (m, 22H, 11CH$_2$), 1.36–1.44 (m, 4H, 2CH$_2$), 1.21 (t, J = 7.2 Hz, 15H, 5CH$_3$), 1.13 (t, J = 7.2 Hz, 3H, 1CH$_3$).

3c: **2** (200 mg, 0.24 mmol), (3,5-difluorophenyl)boronic acid (76.66 mg, 0.49 mmol). **3c**: 181.01 mg, 87%. ^{1}H NMR ($CDCl_3$, TMS, 400 MHz) δ: 7.92 (s, 1H, ArH), 7.87 (s, 1H, ArH), 7.79 (s, 1H, ArH), 7.74 (s, 1H, ArH), 7.15 (s, 1H, ArH), 6.98 (s, 1H, ArH), 6.79 (s, 1H, ArH), 4.18 (t, J = 6.4 Hz, 8H, ArOCH$_2$), 3.70 (t, J = 6.4 Hz, 2H, ArOCH$_2$), 3.35 (t, J = 6.4 Hz, 2H, ArOCH$_2$), 1.88–1.98 (m, 8H, CH$_2$), 1.68–1.75 (m, 2H, CH$_2$), 1.55–1.59 (m, 8H, CH$_2$), 1.37–1.49 (m, 14H, CH$_2$), 1.12–1.21 (m, 4H, CH$_2$), 0.95 (t, J = 7.2 Hz, 15H, CH$_3$), 0.85 (t, J = 7.2 Hz, 3H, CH$_3$).

3d: **2** (200 mg, 0.24 mmol), (3,4,5-trifluorophenyl)boronic acid (85.39 mg, 0.48 mmol). **3d**: 176.31 mg, 83%. ^{1}H NMR ($CDCl_3$, TMS, 400 MHz) δ: 7.91 (s, 1H, 1ArH), 7.85 (s, 1H, 1ArH), 7.78 (s, 1H, ArH), 7.73 (s, 1H, ArH), 7.06 (s, 3H, ArH), 4.18 (t, J = 6.4 Hz, 8H, ArOCH$_2$), 3.70 (t, J = 6 Hz, 2H, ArOCH$_2$), 3.38 (t, J = 6.8 Hz, 2H, ArOCH$_2$), 1.92–1.98 (m, 8H, CH$_2$), 1.70–1.75 (m, 2H, CH$_2$), 1.37–1.49 (m, 22H, CH$_2$), 1.14–1.21 (m, 4H, CH$_2$), 0.93–0.99 (t, J = 7.2 Hz, 15H, CH$_3$), 0.86 (t, J = 7.2 Hz, 3H, CH$_3$). HRMS (m/z) calcd for $C_{54}H_{73}F_3O_6$: 874.5359; found: 874.5348.

3e: **2** (200 mg, 0.24 mmol), (3,4-dichlorophenyl)boronic acid (92.63 mg, 0.48 mmol). **3e**: 177.15 mg, 82%. ^{1}H NMR ($CDCl_3$, TMS, 400 MHz) δ: 7.91 (s, 1H, ArH), 7.86 (s, 1H, ArH), 7.78 (s, 1H, ArH), 7.72 (s, 1H, ArH), 7.63 (d, J = 2 Hz, 1H, ArH), 7.48 (d, J = 8 Hz, 1H, ArH), 7.17 (s, 1H, ArH), 7.07 (s, 1H, ArH), 4.23 (t, J = 6.0 Hz, 6H, 3ArOCH$_2$), 4.16 (t, J = 6.4 Hz, 2H, ArOCH$_2$), 3.58 (t, J = 6.4 Hz, 2H, ArOCH$_2$), 3.22 (t, J = 6.0 Hz, 2H, ArOCH$_2$), 1.86–1.99 (m, 8H, 4CH$_2$), 1.67–1.74 (m, 2H, CH$_2$), 1.53–1.61 (m, 8H, CH$_2$), 1.38–1.48 (m, 14H, CH$_2$), 1.06–1.18 (m, 4H, CH$_2$), 0.94 (t, J = 7.2 Hz, 15H, CH$_3$), 0.85 (t, J = 7.2 Hz, 3H, CH$_3$).

3f: **2** (660 mg, 0.80 mmol), phenylboronic acid (145 mg, 1.2 mmol). **3f**: 620 mg, 94%. ^{1}H NMR ($CDCl_3$, TMS, 400 MHz) δ: 7.88 (d, J = 8.4 Hz, 2H, ArH), 7.83 (s, 1H, ArH), 7.78 (s, 1H, ArH), 7.71 (s, 1H, ArH), 7.39–7.43 (m, 3H, ArH), 7.30–7.35 (s, 1H, ArH), 7.23 (s, 1H, ArH), 4.13–4.27 (t, J = 6.4 Hz, 8H, ArOCH$_2$), 4.14 (t, J = 6.4 Hz, 2H, ArOCH$_2$), 3.59 (t, J = 6.4 Hz, 2H, ArOCH$_2$), 3.15–3.17 (m, 2H, CH$_2$), 1.84–1.99 (m, 10H, CH$_2$), 1.54–1.65 (m, 12H, CH$_2$), 1.34–1.49 (m, 12H, CH$_2$), 0.92–1.00 (t, J = 7.2 Hz, 15H, CH$_3$), 0.81 (t, J = 7.2 Hz, 3H, CH$_3$).

3g: **2** (520 mg, 0.63 mmol), (4-pentylphenyl)boronic acid (144 mg, 0.91 mmol). **3g**: 456 mg, 84%. ^{1}H NMR ($CDCl_3$, TMS, 400 MHz) δ: 7.88 (d, J = 2.8 Hz, 2H, ArH), 7.78 (s, 1H, ArH), 7.71 (s, 1H, ArH), 7.31 (s, 1H, ArH), 7.28 (d, J = 3.6 Hz, 2H, ArH), 7.25 (s, 1H, ArH), 7.22 (s, 1H, ArH), 4.23 (t, J = 6.4 Hz, 6H, ArOCH$_2$), 4.14 (t, J = 6.4 Hz, 2H, ArOCH$_2$), 3.58 (t, J = 6.4 Hz, 2H, ArOCH$_2$), 3.18 (t, J = 6.4 Hz, 2H, ArOCH$_2$), 2.64 (t, J = 8.0 Hz, 2H, ArCH$_2$), 1.85–1.99 (m, 8H, CH$_2$), 1.57–1.69 (m, 12H, CH$_2$), 1.33–1.49 (m, 18H, CH$_2$), 1.03–1.17 (m, 4H, CH$_2$), 0.93 (t, J = 7.2 Hz, 18H, CH$_3$), 0.80 (t, J = 7.2 Hz, 3H, CH$_3$).

3h: **2** (800 mg, 0.97 mmol), (3,4-bis(pentyloxy)phenyl)boronic acid (429 mg, 1.46 mmol). **3h**: 900 mg, 93%. ^{1}H NMR ($CDCl_3$, TMS, 400 MHz) δ: 7.88 (s, 2H, ArH), 7.78 (s, 1H, ArH), 7.71 (s, 1H, ArH), 7.34 (s, 1H, ArH), 6.98 (d, J = 2.0 Hz, 1H, ArH), 6.91 (d, J = 8.4 Hz, 1H, ArH), 6.83 (s, 1H, ArH), 4.23 (t, J = 6.4 Hz, 6H, ArOCH$_2$), 4.15 (t, J = 6.8 Hz, 2H, ArOCH$_2$), 3.85 (t, J = 6.4 Hz, 4H, ArOCH$_2$), 3.63 (t, J = 6.4 Hz, 1H, ArOCH$_2$), 3.53 (t, J = 6.8 Hz, 1H, ArOCH$_2$), 3.26 (t, J = 6.4 Hz, 2H, 1ArOCH$_2$), 1.83–1.99 (m, 10H, CH$_2$), 1.72–1.79 (m, 2H, CH$_2$), 1.61–1.67 (m, 2H, CH$_2$), 1.55–1.60 (m, 10H, CH$_2$), 1.30–1.50 (m, 20H, CH$_2$), 1.09–1.20 (m, 4H, CH$_2$), 0.88 (t, J = 7.2 Hz, 21H, CH$_3$), 0.82 (t, J = 6.8 Hz, 3H, CH$_3$).

3i: **2** (500 mg, 0.61 mmol), (3,4-dimethoxyphenyl)boronic acid (166 mg, 0.91 mmol). **3i**: 427 mg, 80%. ^{1}H NMR ($CDCl_3$, TMS, 400 MHz) δ: 7.93 (d, J = 4.0 Hz, 2H, ArH), 7.83 (s, 1H, ArH), 7.77 (s, 1H, ArH), 7.37 (s, 1H, ArH), 7.06 (s, 1H, ArH), 6.93 (s, 2H, ArH), 4.28 (t, J = 6.8 Hz, 6H, ArOCH$_2$), 4.20 (t, J = 6.8 Hz, 2H, ArOCH$_2$), 3.97 (s, 3H, ArOCH$_3$), 3.85 (s, 3H, ArOCH$_3$), 3.72 (t, J = 6.4 Hz, 1H, ArOCH$_2$), 3.58 (t, J = 6.8 Hz, 1H, ArOCH$_2$), 3.30 (t, J = 6.8 Hz, 2H, ArOCH$_2$), 1.90–2.04 (m, 8H, CH$_2$), 1.66–1.72 (m, 2H, CH$_2$), 1.60–1.63 (m, 8H, CH$_2$), 1.45–1.55 (m, 10H, CH$_2$), 1.38–1.41 (m, 4H, CH$_2$), 1.12–1.24 (m, 4H, CH$_2$), 0.96 (t, J = 7.2 Hz, 15H, CH$_3$), 0.87 (t, J = 6.8 Hz, 3H, CH$_3$).

3j: **2** (200 mg, 0.24 mmol), (4-methoxyphenyl)boronic acid (73.77 mg, 0.48 mmol). **3j**: 179.75 mg, 87%. ^{1}H NMR ($CDCl_3$, TMS, 400 MHz) δ: 7.88 (d, J = 6.4 Hz, 2H, ArH), 7.78 (s, 1H, ArH), 7.72 (s, 1H, ArH), 7.30 (s, 3H, ArH), 6.97 (d, J = 8.8 Hz, 2H, ArH), 4.16–4.26 (t, J = 6.4 Hz, 8H, ArOCH$_2$), 3.85 (s, 3H, ArOCH$_3$), 3.60 (t, J = 6.4 Hz, 2H, ArOCH$_2$), 3.27 (t, J = 6.4 Hz, 2H, ArOCH$_2$), 1.94–1.98 (m, 10H, CH$_2$), 1.35–1.58 (m, 24H, CH$_2$), 1.08–1.16 (m, 2H, CH$_2$), 0.93–1.00 (t, J = 7.2 Hz, 15H, CH$_3$), 0.82 (t, J = 7.2 Hz, 3H, CH$_3$).

3k: **2** (500 mg, 0.61 mmol), *p*-tolylboronic acid (165 mg, 1.21 mmol). **3k**: 430.79 mg, 85%. ^{1}H NMR ($CDCl_3$, TMS, 400 MHz) δ: 7.91 (d, J = 4.4 Hz, 2H, ArH), 7.81 (s, 1H, ArH), 7.74 (s, 1H, ArH), 7.29 (d, J = 6.4 Hz, 2H, ArH), 7.25 (s, 3H, ArH), 4.24 (t, J = 6.4 Hz, 6H, ArOCH$_2$), 4.17 (t, J = 6.4 Hz, 2H, ArOCH$_2$), 3.64 (t, J = 6.4 Hz, 2H, ArOCH$_2$), 3.21 (t, J = 6.8 Hz, 2H, ArOCH$_2$), 2.43 (s, 3H, ArCH$_3$),

1.89–2.00 (m, 8H, CH_2), 1.47–1.59 (m, 12H, CH_2), 1.37–1.45 (m, 12H, CH_2), 1.07–1.16 (m, 4H, CH_2), 0.95 (t, J = 6.4 Hz, 15H, CH_3), 0.83 (t, J = 7.2 Hz, 3H, CH_3).

3l: **2** (100 mg, 0.12 mmol), (4-cyanophenyl)boronic acid (35.67 mg, 0.24 mmol). **3l**: 97.56 mg, 95%. ^{1}H NMR ($CDCl_3$, TMS, 400 MHz) δ: 7.93 (s, 1H, ArH), 7.86 (s, 1H, ArH), 7.75 (d, J = 9.6 Hz, 2H, ArH), 7.72 (s, 2H, ArH), 7.56 (d, J = 8.4 Hz 2H, ArH), 6.90 (s, 1H, ArH), 4.22 (t, J = 6.4 Hz, 6H, $ArOCH_2$), 4.15 (t, J = 6.8 Hz, 2H, $ArOCH_2$), 3.62 (t, J = 6.4 Hz, 2H, $ArOCH_2$), 3.14 (t, J = 6.8 Hz, 2H, $ArOCH_2$), 1.87–1.98 (m, 8H, CH_2), 1.64–1.71 (m, 2H, CH_2), 1.55–1.59 (m, 10H, CH_2), 1.36–1.50 (m, 14H, CH_2), 1.12–1.18 (m, 2H, CH_2), 0.92 (t, J = 7.2 Hz, 15H, CH_3), 0.83 (t, J = 7.2 Hz, 3H, CH_3). HRMS (m/z) calcd for $C_{55}H_{75}NO_6$: 845.5594; found: 845.5586.

3m: **2** (500 mg, 0.61 mmol), naphthalene-2-ylboronic acid (208 mg, 1.21 mmol). **3m**: 450 mg, 85%. ^{1}H NMR ($CDCl_3$, TMS, 400 MHz) δ: 7.94 (d, J = 6.4 Hz, 2H, ArH), 7.91 (s, 1H, ArH), 7.88 (s, 1H, ArH), 7.86 (d, J = 7.2 Hz, 1H, ArH), 7.78–7.79 (m, 2H, ArH), 7.71 (s, 1H, ArH), 7.44–7.50 (s, 3H, ArH), 7.15 (s, 1H, ArH), 4.22 (t, J = 6.4 Hz, 6H, $ArOCH_2$), 4.11 (t, J = 6.4 Hz, 2H, $ArOCH_2$), 3.55 (t, J = 6.4 Hz, 2H, $ArOCH_2$), 2.51 (t, J = 6.4 Hz, 2H, $ArOCH_2$), 1.92–2.00 (m, 6H, CH_2), 1.82–1.86 (m, 2H, CH_2), 1.55–1.60 (m, 8H, CH_2), 1.43–1.48 (m, 10H, CH_2), 1.20–1.28 (m, 4H, CH_2), 1.06–1.21 (m, 2H, CH_2), 0.95–1.00 (m, 4H, CH_2), 0.81 (t, J = 7.2 Hz, 15H, CH_3), 0.53 (t, J = 7.2 Hz, 3H, CH_3). HRMS (m/z) calcd for $C_{58}H_{78}O_6$: 870.5798; found: 870.5795.

3n: **2** (100 mg, 0.12 mmol), thiophen-3ylboronic acid (31 mg, 0.24 mmol). **3n**: 79.3 mg, 79%. ^{1}H NMR ($CDCl_3$, TMS, 400 MHz) δ: 7.89 (d, J = 6.0 Hz, 2H, ArH), 7.86 (s, 2H, ArH), 7.81 (s, 1H, ArH), 7.75 (s, 1H, ArH), 7.36 (s, 1H, ArH), 7.28 (s, 1H, ArH), 4.24 (t, J = 6.4 Hz, 6H, $ArOCH_2$), 4.19 (t, J = 6.4 Hz, 2H, $ArOCH_2$), 3.66 (t, J = 6.4 Hz, 2H, $ArOCH_2$), 3.47 (t, J = 6.4 Hz, 2H, $ArOCH_2$), 1.90–2.01 (m, 8H, CH_2), 1.55–1.63 (m, 12H, CH_2), 1.40–1.53 (m, 12H, CH_2), 1.19–1.24 (m, 4H, CH_2), 0.95–1.02 (t, J = 7.2 Hz, 15H, CH_3), 0.88 (t, J = 7.2 Hz, 3H, CH_3). HRMS (m/z) calcd for $C_{52}H_{74}O_6S$: 826.5206; found: 826.5195.

4a: to a solution of **3a** (310 mg, 0.37 mmol) in dry CH_2Cl_2 (15 mL), $FeCl_3$ (600.28 mg, 3.69 mmol) and a drop of concentrated H_2SO_4 were added; the mixture was stirred at room temperature for 40 min. Then, methanol (2 mL) and water (2 mL) were added. After extraction with CH_2Cl_2, the organic extracts were washed with a saturated NaCl solution, dried over $MgSO_4$, filtered, and concentrated *in vacuo* to give a residue. DMF (20 mL) was added to the residue, followed by 1-bromopentane (334.68 mg, 2.22 mmol), K_2CO_3 powder (509.79 mg, 3.69 mmol) and zinc powder (500 mg). The mixture was stirred at 80 °C for 16 h. After the reaction mixture was cooled, it was filtered through a thin layer of silica gel and the solvent was concentrated *in vacuo*. The residue was purified by silica gel column chromatography, eluted with light petroleum ether/CH_2Cl_2 (3 : 2, v/v) and recrystallized from ethanol to yield a white solid, **4a** (184.8 mg, 60%). ^{1}H NMR ($CDCl_3$, TMS, 400 MHz) δ: 9.68 (s, 1H, ArH), 9.47 (s, 1H, ArH), 8.15 (d, J = 14.8 Hz, 2H, ArH), 7.96 (s, 2H, ArH), 7.34 (s, 1H, ArH), 4.36 (t, J = 6.4 Hz, 8H, $ArOCH_2$), 4.03 (t, J = 6.4 Hz, 4H, $ArOCH_2$), 1.89–2.05 (m, 12H, CH_2), 1.38–1.63 (m, 24H, CH_2), 1.02 (t, J = 7.2 Hz, 18H, CH_3). HRMS (m/z) calcd for $C_{54}H_{73}FO_6$: 836.5391; found: 836.5385.

All the other dibenzo[*fg*,*op*]tetracene discogens were prepared and purified accordingly.

4b: **3b** (200 mg, 0.22 mmol), $FeCl_3$ (364. 8 mg, 2.24 mmol); zinc powder (400 mg); 1-bromopentane (270 mg, 1.79 mmol), K_2CO_3 (309 mg, 2.24 mmol). **4b**: 97.83 mg, 52%. ^{1}H NMR ($CDCl_3$, TMS, 400 MHz) δ: 9.62 (s, 2H, ArH), 8.10 (s, 2H, ArH), 7.91 (s, 2H, ArH), 4.34 (t, J = 6.4 Hz, 8H, OCH_2), 3.98 (t, J = 6.4 Hz, 4H, OCH_2), 1.90–2.05 (m, 12H, CH_2), 1.41–1.63 (m, 24H, CH_2), 1.03 (t, J = 7.2 Hz, 18H, CH_3). ^{13}C NMR ($CDCl_3$, 100 MHz) δ: 151.06, 150.10, 149.95, 149.64, 147.63, 147.48, 144.94, 127.72, 127.67, 127.62, 124.64, 123.79, 121.86, 119.61, 116.18, 116.10, 116.05, 115.97, 107.27, 106.58, 77.35, 77.03, 76.71, 73.79, 69.59, 69.32, 30.14, 29.37, 29.13, 28.52, 28.47, 28.41, 22.63, 14.15, 14.06. HRMS (m/z) calcd for $C_{54}H_{72}F_2O_6$: 854.5297; found: 854.5284.

4c: **3c** (220 mg, 0.25 mmol), $FeCl_3$ (409.41 mg, 2.52 mmol); zinc powder (400 mg); 1-bromopentane (228.26 mg, 1.51 mmol), K_2CO_3 powder (347.68 mg, 2.52 mmol). **4c**: 43.77 mg, 40%. ^{1}H NMR ($CDCl_3$, TMS, 400 MHz) δ: 9.25 (s, 1H, ArH), 8.04 (s, 2H, ArH), 7.91 (s, 2H, ArH), 7.08 (s, 1H, ArH), 4.34 (t, J = 6.4 Hz, 8H, $ArOCH_2$), 4.04 (t, J = 6.8 Hz, 2H, $ArOCH_2$), 3.85 (t, J = 6.4 Hz, 2H, $ArOCH_2$), 1.96–2.02 (m, 10H, CH_2), 1.57–1.62 (m, 12H, CH_2), 1.34–1.50 (m, 12H, CH_2), 1.21–1.25 (m, 2H, CH_2), 1.02 (t, J = 7.2 Hz, 15H, CH_3), 0.85 (t, J = 7.6 Hz, 3H, CH_3). HRMS (m/z) calcd for $C_{54}H_{72}F_2O_6$: 854.5297; found: 854.5291.

4e: **3e** (300 mg, 0.34 mmol), $FeCl_3$ (547.7 mg, 3.37 mmol); zinc powder (500 mg); 1-bromopentane (305.37 mg, 2.02 mmol), K_2CO_3 powder (465.14 mg, 3.37 mmol). **4e**: 142 mg, 47.5%. ^{1}H NMR ($CDCl_3$, TMS, 400 MHz) δ: 9.92 (s, 2H, ArH), 8.14 (s, 2H, ArH), 7.94 (s, 2H, ArH), 4.34 (t, J = 6.4 Hz, 4H, $ArOCH_2$), 4.28 (t, J = 6.4 Hz, 4H, $ArOCH_2$), 3.99 (t, J = 6.4 Hz, 4H, $ArOCH_2$), 1.91–2.05 (m, 12H, CH_2), 1.52–1.64 (m, 12H, CH_2), 1.42–1.51 (m, 12H, CH_2), 1.01 (t, J = 7.2 Hz, 18H, CH_3). HRMS (m/z) calcd for $C_{54}H_{72}Cl_2O_6$: 886.4706; found: 886.4708.

4f: **3f** (100 mg, 0.12 mmol), $FeCl_3$ (189.65 mg, 1.16 mmol); zinc powder (200 mg); 1-bromopentane (270 mg, 1.79 mmol), K_2CO_3 (309 mg, 2.24 mmol). **4f**: 60.54 mg, 62%. ^{1}H NMR ($CDCl_3$, TMS, 400 MHz) δ: 9.68 (d, J = 6.4 Hz, 2H, ArH), 8.12 (s, 2H, ArH), 7.96 (s, 2H, ArH), 7.57–7.61 (m, 2H, ArH), 4.36 (t, J = 6.4 Hz, 8H, OCH_2), 3.98 (t, J = 6.4 Hz, 4H, OCH_2), 1.87–2.03 (m, 12H, CH_2), 1.38–1.63 (m, 24H, CH_2), 1.02 (t, J = 7.2 Hz, 18H, CH_3). HRMS (m/z) calcd for $C_{54}H_{74}O_6$: 818.5485; found: 818.5377.

4g: **3g** (656 mg, 0.73 mmol), $FeCl_3$ (788.6 mg, 7.28 mmol); zinc powder (500 mg); 1-bromopentane (881.84 mg, 5.84 mmol), K_2CO_3 (1.01 g, 7.3 mmol). **4g**: 324.6 mg, 50%. ^{1}H NMR ($CDCl_3$, TMS, 400 MHz) δ: 9.58 (s, 1H, ArH), 9.52 (s, 1H, ArH), 8.11 (d, J = 6.4 Hz, 2H, ArH), 7.96 (s, 2H, ArH), 7.44 (s, 1H, ArH), 4.34 (t, J = 6.4 Hz, 8H, OCH_2), 4.00 (t, J = 6.4 Hz, 4H, OCH_2), 2.82–2.84 (m, 2H, CH_2), 1.90–2.04 (m, 12H, CH_2), 1.76–1.82 (m, 2H, CH_2), 1.37–1.59 (m, 28H, CH_2), 0.94–1.00 (t, J = 7.2 Hz, 21H, CH_3). HRMS (m/z) calcd for $C_{59}H_{84}O_6$: 888.6268; found: 888.6265.

4h: **3h** (200 mg, 0.21 mmol), $FeCl_3$ (341.3 mg, 2.1 mmol); zinc powder (400 mg); 1-bromopentane (190.26 mg, 1.26 mmol), K_2CO_3 (289.8 mg, 2.1 mmol). **4h**: 157 mg, 75%. ^{1}H NMR ($CDCl_3$, TMS, 400 MHz) δ: 9.27 (s, 2H, ArH), 8.10 (s, 2H, ArH), 7.98

(s, 2H, ArH), 4.35 (t, J = 6.4 Hz, 4H, $ArOCH_2$), 4.29 (t, J = 6.8 Hz, 4H, $ArOCH_2$), 4.23 (t, J = 6.4 Hz, 4H, $ArOCH_2$), 3.97 (t, J = 6.8 Hz, 4H, $ArOCH_2$), 1.89–2.09 (m, 16H, CH_2), 1.35–1.67 (m, 32H, CH_2), 1.02 (t, J = 7.2 Hz, 24H, CH_3). ^{13}C NMR ($CDCl_3$, 100 MHz) δ: 14.05, 14.10, 14.13, 22.56, 22.59, 22.63, 22.71, 28.34, 28.39, 28.52, 29.10, 29.14, 29.37, 30.35, 68.82, 69.14, 69.65, 76.70, 77.01, 77.33, 111.21, 111.24, 111.25, 119.56, 124.49, 124.52, 124.54, 147.98, 148.04, 149.47, 149.50, 149.55. Elemental analysis calcd for $C_{96}H_{130}F_8O_{16}$: C, 77.53; H, 9.56; found: C, 77.37; H, 9.56. HRMS (m/z) calcd for $C_{64}H_{94}O_8$: 990.6949; found: 990.6942.

4i: **3i** (200 mg, 0.23 mmol), $FeCl_3$ (373.75 mg, 2.3 mmol); zinc powder (400 mg); 1-bromopentane (208.38 mg, 1.38 mmol), K_2CO_3 (317.4 mg, 2.3 mmol). **4i**: 131 mg, 65%. ^{1}H NMR ($CDCl_3$, TMS, 400 MHz) δ: 9.30 (s, 2H, ArH), 8.11 (s, 2H, ArH), 7.98 (s, 2H, ArH), 4.36 (t, J = 6.4 Hz, 4H, $ArOCH_2$), 4.29 (t, J = 6.8 Hz, 4H, $ArOCH_2$), 4.10 (s, 6H, $ArOCH_3$), 3.98 (t, J = 6.8 Hz, 4H, $ArOCH_2$), 1.91–2.07 (m, 12H, CH_2), 1.60–1.68 (m, 8H, CH_2), 1.47–1.53 (m, 12H, CH_2), 1.35–1.40 (m, 4H, CH_2), 0.97–1.02 (m, 12H, CH_3), 0.92 (t, J = 7.2 Hz, 6H, CH_3). ^{13}C NMR ($CDCl_3$, 100 MHz) δ: 14.05, 14.13, 22.59, 22.63, 22.66, 28.35, 28.39, 28.51, 29.13, 29.35, 30.35, 55.81, 69.14, 69.65, 73.99, 76.69, 77.00, 77.33, 105.17, 107.53, 109.59, 119.52, 123.04, 124.04, 124.57, 124.74, 144.34, 147.91, 149.53, 150.94. HRMS (m/z) calcd for $C_{56}H_{78}O_8$ $[MH]^+$: 879.5697; found: 879.5771.

4j: **3j** (150 mg, 0.18 mmol), $FeCl_3$ (286.35 mg, 1.76 mmol); zinc powder (200 mg); 1-bromopentane (159.65 mg, 1.06 mmol), K_2CO_3 (243.19 mg, 1.76 mmol). **4j**: 89.78 mg, 60%. ^{1}H NMR ($CDCl_3$, TMS, 400 MHz) δ: 9.66 (d, J = 9.6 Hz, 1H, ArH), 9.31 (d, J = 2.4 Hz, 1H, ArH), 8.17 (s, 1H, ArH), 8.12 (s, 1H, ArH), 8.00 (s, 2H, ArH), 7.29 (s, 1H, ArH), 4.40 (t, J = 6.4 Hz, 8H, $ArOCH_2$), 4.05 (t, J = 6.4 Hz, 4H, $ArOCH_2$), 4.04 (s, 3H, $ArOCH_3$), 1.92–2.12 (m, 12H, CH_2), 1.41–1.69 (m, 24H, CH_2), 1.06 (t, J = 7.2 Hz, 18H, CH_3). HRMS (m/z) calcd for $C_{55}H_{76}O_7$: 848.5591; found: 848.5588.

4k: **3k** (300 mg, 0.36 mmol), $FeCl_3$ (583.68 mg, 3.59 mmol); zinc powder (400 mg); 1-bromopentane (325.42 mg, 2.15 mmol), K_2CO_3 (495.69 mg, 3.59 mmol). **4k**: 183.3 mg, 61%. ^{1}H NMR ($CDCl_3$, TMS, 400 MHz) δ: 9.59 (s, 2H, ArH), 8.14 (d, J = 7.2 Hz, 2H, ArH), 8.00 (s, 2H, ArH), 7.45 (s, 1H, ArH), 4.40 (t, J = 6.4 Hz, 8H, $ArOCH_2$), 4.02 (t, J = 6.4 Hz, 4H, $ArOCH_2$), 2.61 (s, 3H, $ArCH_3$), 2.00–2.09 (m, 8H, CH_2), 1.90–1.98 (m, 4H, CH_2), 1.60–1.69 (m, 12H, CH_2), 1.43–1.57 (m, 12H, CH_2), 1.06 (t, J = 7.2 Hz, 18H, CH_3). HRMS (m/z) calcd for $C_{55}H_{76}O_6$: 832.5642; found: 832.5641.

4n: to a stirred solution of **3n** (115 mg, 0.14 mmol) in CH_2Cl_2 (105 mL) at 0 °C, a solution of $FeCl_3$ (67.8 mg, 0.42 mmol) in $MeNO_2$ (1.5 mL) was added under argon atmosphere and stirred at 0 °C for 1.5 h. Then, cold methanol (2 mL) and water (2 mL) were added to quench the reaction and the mixture was extracted in CH_2Cl_2. The residue was purified by silica gel column chromatography, eluted with petroleum ether/dichloromethane (3 : 2, v/v) and crystallized in ethanol to yield the product (44 mg, 38%). Repeated purification by column chromatography and re-crystallization resulted in the oxidation of the product to a black powder. ^{1}H NMR ($CDCl_3$, TMS, 400 MHz) δ: 8.86 (s, 1H, ArH), 8.22 (s, 1H, ArH), 8.17 (s, 1H, ArH), 8.05 (s, 1H, ArH), 8.00 (s, 1H, ArH), 7.69 (s, 1H, ArH), 4.60 (t, J = 6.4 Hz, 12H, $ArOCH_2$), 1.90–2.20 (m, 12H, CH_2), 1.40–1.80 (m, 24H, CH_2), 1.10 (t, J = 7.2 Hz, 18H, CH_3).

Acknowledgements

This research was financially supported by the National Natural Science Foundation of China (grant no. 51273133, and 51443004). BD and BH thank the CNRS and the University of Strasbourg for support.

References

1 (*a*) L. Schmidt-Mende, A. Fechtenkötter, K. Müllen, E. Moons, R. H. Friend and J. D. MacKenzie, *Science*, 2001, **293**, 1119–1122; (*b*) J. Idé, R. Méreau, L. Ducasse, F. Castet, H. Bock, Y. Olivier, J. Cornil, D. Beljonne, G. D'Avino, O. M. Roscioni, L. Muccioli and C. Zannoni, *J. Am. Chem. Soc.*, 2014, **136**, 2911–2920.

2 (*a*) N. Boden, R. J. Bushby, J. Clements and B. Movaghar, *J. Mater. Chem.*, 1999, **9**, 2081–2086; (*b*) I. Seguy, P. Jolinat, P. Destruel, J. Farenc, R. Mamy, H. Bock, J. Ip and T. P. Nguyen, *J. Appl. Phys.*, 2001, **89**, 5442–5448; (*c*) M. Oukachmih, P. Destruel, L. Seguy, G. Ablart, P. Jolinat, S. Archambeau, M. Mabiala, S. Fouet and H. Bock, *Sol. Energy Mater. Sol. Cells*, 2005, **85**, 535–543.

3 N. Boden, R. J. Bushby, J. Clements, M. V. Jesudason, P. F. Knowles and G. Williams, *Chem. Phys. Lett.*, 1988, **152**, 94–99.

4 (*a*) D. Adam, P. Schuhmacher, J. Simmerer, L. Häussling, K. Siemensmeyer, K. H. Etzbachi, H. Ringsdorf and D. Haarer, *Nature*, 1994, **371**, 141–143; (*b*) W. Pisula, M. Kastler, D. Wasserfallen, M. Mondeshki, J. Piris, I. Schnell and K. Müllen, *Chem. Mater.*, 2006, **18**, 3634–3640; (*c*) J. Wu, W. Pisula and K. Mullen, *Chem. Rev.*, 2007, **107**, 718–747; (*d*) X. Feng, V. Marcon, W. Pisula, M. R. Hansen, J. Kirkpatrick, F. Grozema, D. Andrienko, K. Kremer and K. Müllen, *Nat. Mater.*, 2009, **8**, 421–426; (*e*) W. Pisula, X. Feng and K. Mullen, *Chem. Mater.*, 2011, **23**, 554–567.

5 (*a*) S. Kumar, *Liq. Cryst.*, 2004, **31**, 1037–1059; (*b*) T. Kato, T. Yasuda and Y. Kamikawa, *Chem. Commun.*, 2009, 729–739; (*c*) R. J. Bushby and K. Kawata, *Liq. Cryst.*, 2011, **38**, 1415–1426; (*d*) B. Roy, N. De and K. C. Majumdar, *Chem. – Eur. J.*, 2012, **18**, 14560–14588.

6 (*a*) H. Eichhorn, *J. Porphyrins Phthalocyanines*, 2000, **4**, 88–102; (*b*) T. Wöhrle, I. Wurzbach, J. Kirres, A. Kostidou, N. Kapernaum, J. Litterscheidt, J. Christian Haenle, P. Staffeld, A. Baro, F. Giesselmann and S. Laschat, *Chem. Rev.*, 2016, **116**, 1139–1241.

7 (*a*) S. Sergeyev, W. Pisula and Y. H. Geerts, *Chem. Soc. Rev.*, 2007, **36**, 1902–1929; (*b*) Y. Shimizu, K. Oikawa, K. I. Nakayama and D. Guillon, *J. Mater. Chem.*, 2007, **17**, 4223–4229; (*c*) S. Xiao, M. Myers, Q. Miao, S. Sanaur, K. Pang, M. L. Steigerwald and C. Nuckolls, *Angew. Chem., Int. Ed.*, 2005, **44**, 7390–7394; (*d*) M. O'Neill and S. M. Kelly, *Adv. Mater.*, 2003, **15**, 1135–1146; (*e*) B. R. Kaafarani, *Chem. Mater.*, 2011, **23**, 378–396.

8 (*a*) T. Kushida, A. Shuto, M. Yoshio, T. Kato and S. Yamaguchi, *Angew. Chem., Int. Ed.*, 2015, **54**, 6922–6925; (*b*) T. Yasuda, T. Shimizu, F. Liu, G. Ungar and T. Kato, *J. Am. Chem. Soc.*, 2011, **133**, 13437–13444; (*c*) X. Liu, T. Usui, H. Iino and J. Hanna, *J. Mater. Chem. C*, 2013, **1**, 8186–8193; (*d*) X. Y. Liu, T. Usui and J. Hanna, *Chem. Mater.*, 2014, **26**, 5437–5440; (*e*) X. Y. Liu, T. Usui and J. Hanna, *Chem. – Eur. J.*, 2014, **20**, 14207–14212; (*f*) H. Iino, J. I. Hanna, R. J. Bushby, B. Movaghar, B. J. Whitaker and M. J. Cook, *Appl. Phys. Lett.*, 2005, **87**, 132102; (*g*) M. Funahashi and A. Sonoda, *Org. Electron.*, 2012, **13**, 1633–1640.

9 (*a*) H. Monobe and Y. Shimizu, *Jpn. J. Appl. Phys.*, 2014, **53**, 01AE06; (*b*) K. Q. Zhao, C. Chen, H. Monobe, P. Hu, B. Q. Wang and Y. Shimizu, *Chem. Commun.*, 2011, **47**, 6290–6292; (*c*) L. Sosa-Vargas, F. Nekelson, D. Okuda, M. Takahashi, Y. Matsuda, Q. D. Dao, Y. Hiroyuki, A. Fujii, M. Ozaki and Y. Shimizu, *J. Mater. Chem. C*, 2015, **3**, 1757–1765; (*d*) K. Q. Zhao, L. L. An, X. B. Zhang, W. H. Yu, P. Hu, B. Q. Wang, J. Xu, Q. D. Zeng, H. Monobe, Y. Shimizu, B. Heinrich and B. Donnio, *Chem. – Eur. J.*, 2015, **21**, 10379–10390; (*e*) S. Mery, D. Haristoy, J. Nicoud, D. Guillon, S. Diele, H. Monobe and Y. Shimizu, *J. Mater. Chem.*, 2002, **12**, 37–41.

10 (*a*) M. Kastler, F. Laquai, K. Mullen and G. Wegner, *Appl. Phys. Lett.*, 2006, **89**, 252103; (*b*) A. Demenev, S. H. Eichhorn, T. Taerum, D. F. Perepichka, S. Patwardhan, F. C. Grozema, L. D. A. Siebbeles and R. Klenkler, *Chem. Mater.*, 2010, **22**, 1420–1428.

11 (*a*) A. M. Van de Craats and J. M. Warman, *Adv. Mater.*, 2001, **13**, 130–133; (*b*) M. G. Debije, J. Piris, M. P. de Haas, J. M. Warman, Z. Tomovic, C. D. Simpson, M. D. Watson and K. Mullen, *J. Am. Chem. Soc.*, 2004, **126**, 4641–4645.

12 (*a*) N. Miyaura, K. Yamada and A. Suzuki, *Tetrahedron Lett.*, 1979, **20**, 3437; (*b*) N. Miyaura and A. Suzuki, *J. Chem. Soc., Chem. Commun.*, 1979, 866–867; (*c*) A. Suzuki, *Angew. Chem., Int. Ed.*, 2011, **50**, 6722–6737.

13 (*a*) K. Sonogashira, Y. Tohda and N. Hagihara, *Tetrahedron Lett.*, 1975, **16**, 4467–4470; (*b*) T. Hirose, Y. Miyazaki, M. Watabe, S. Akimoto, T. Tachikawa, K. Kodama and M. Yasutake, *Tetrahedron*, 2015, **71**, 4714–4721; (*c*) X. Zhang, H. Wang, S. Wang, Y. Shen, Y. Yang, K. Deng, K. Zhao, Q. Zeng and C. Wang, *J. Phys. Chem. C*, 2013, **117**, 307–312; (*d*) Y. Geng, S. Chang, K. Zhao, Q. Zeng and C. Wang, *J. Phys. Chem. C*, 2015, **119**, 18216–18220; (*e*) S. Thiery, B. Heinrich, B. Donnio, C. Poriel and F. Camerel, *J. Phys. Chem. C*, 2015, **119**, 10564–10575.

14 R. Scholl and J. Mansfeld, *Ber. Dtsch. Chem. Ges.*, 1910, **43**, 1734–1746.

15 (*a*) P. Kovacic and M. B. Jones, *Chem. Rev.*, 1987, **87**, 357–379; (*b*) D. Perez and E. Guitian, *Chem. Soc. Rev.*, 2004, **33**, 274–283; (*c*) A. A. Sarhan and C. Bolm, *Chem. Soc. Rev.*, 2009, **38**, 2730–2744; (*d*) M. Grzybowski, K. Skonieczny, H. Butenschon and D. T. Gryko, *Angew. Chem., Int. Ed.*, 2013, **52**, 9900–9930; (*e*) S. R. Waldvogel and S. Trosien, *Chem. Commun.*, 2012, **48**, 9109–9119.

16 (*a*) H. Bengs, O. Karthaus, H. Ringsdorf, C. Baehr, M. Ebert and J. H. Wendorff, *Liq. Cryst.*, 1991, **10**, 161–168; (*b*) N. Boden, R. C. Borner, R. J. Bushby, A. N. Cammidge and M. V. Jesudason, *Liq. Cryst.*, 1993, **15**, 851–858; (*c*) C. Feng, X. Tian, J. Zhou, S. Xiang, W. Yu, B. Wang, P. Hu, C. Redshaw and K. Zhao, *Org. Biomol. Chem.*, 2014, **12**, 6977–6981.

17 (*a*) Q. Zhang, P. Prins, S. C. Jones, S. Barlow, T. Kondo, Z. An, L. D. A. Siebbeles and S. R. Marder, *Org. Lett.*, 2005, **7**, 5019–5022; (*b*) S. H. Wadumethrige and R. Rathore, *Org. Lett.*, 2008, **10**, 5139–5142; (*c*) X. Feng, W. Pisula, M. Takase, X. Dou, V. Enkelmann, M. Wagner, N. Ding and K. Mullen, *Chem. Mater.*, 2008, **20**, 2872–2874.

18 (*a*) L. Chen, S. R. Puniredd, Y. Tan, M. Baumgarten, U. Zschieschang, V. Enkelmann, W. Pisula, X. Feng, H. Klauk and K. Mullen, *J. Am. Chem. Soc.*, 2012, **134**, 17869–17872; (*b*) Q. Xaio, T. Sakurai, T. Fukino, K. Akaike, Y. Honsho, A. Saeki, S. Seki, K. Kato, M. Takata and T. Aida, *J. Am. Chem. Soc.*, 2013, **135**, 18268–18271; (*c*) J. Luo, B. Zhao, H. S. O. Chan and C. Chi, *J. Mater. Chem.*, 2010, **20**, 1932–1941; (*d*) J. Luo, B. Zhao, J. Shao, K. A. Lim, H. S. O. Chan and C. Chi, *J. Mater. Chem.*, 2009, **19**, 8327–8334; (*e*) Q. Ye, J. Chang, K. Huang and C. Chi, *Org. Lett.*, 2011, **13**, 5960–5963.

19 M. C. Artal, K. J. Toyne, J. W. Goodby, J. Barbera and D. J. Photinos, *J. Mater. Chem.*, 2001, **11**, 2801–2807.

20 D. Myśliwiec, B. Donnio, P. J. Chmielewski, B. Heinrich and M. Stepień, *J. Am. Chem. Soc.*, 2012, **134**, 4822–4833.

21 B. Zhao, B. Liu, R. Q. Png, K. Zhang, K. A. Lim, J. Luo, J. Shao, P. K. H. Ho, C. Chi and J. Wu, *Chem. Mater.*, 2010, **22**, 435–449.

22 T. Wohrle, J. Kirres, M. Kaller, M. Mansueto, S. Tussetschlager and S. Laschat, *J. Org. Chem.*, 2014, **79**, 10143–10152.

23 (*a*) S. Kumar and M. Manickam, *Chem. Commun.*, 1997, 1615–1666; (*b*) S. Kumar and S. Varshney, *Liq. Cryst.*, 1999, **26**, 1841–1843; (*c*) S. Kumar and H. T. Srinivasa, *Org. Chem.: Curr. Res.*, 2013, **2**, 1000116; (*d*) T. Yang, J. Pu, J. Zhang and W. Wang, *J. Org. Chem.*, 2013, **78**, 4857–4866.

24 (*a*) D. J. Gregg, C. M. A. Ollagnier, C. M. Fitchett and S. M. Draper, *Chem. – Eur. J.*, 2006, **12**, 3043–3052; (*b*) X. Dou, X. Yang, G. J. Bodwell, M. Wagner, V. Enkelmann and K. Mullen, *Org. Lett.*, 2007, **9**, 2485–2488; (*c*) S. H. Wadumethrige and R. Rathore, *Org. Lett.*, 2008, **10**, 5139–5142.

25 (*a*) Y. Lu and J. S. Moore, *Tetrahedron Lett.*, 2009, **50**, 4071–4077; (*b*) S. Nagarajan, C. Barthes and A. Gourdon, *Tetrahedron*, 2009, **65**, 3767–3772.

26 (*a*) W. Xiao, Z. He, M. Xu, N. Wu, X. Kong and X. Jing, *Tetrahedron Lett.*, 2015, **56**, 700–705; (*b*) H. Wu, C. Zhang, J. Pu and Y. Wang, *Liq. Cryst.*, 2014, **41**, 1173–1178; (*c*) R. J. Bushby and Z. Lu, *Synthesis*, 2001, 763–767; (*d*) S. Kumar and B. Lakshmi, *Tetrahedron Lett.*, 2005, **46**, 2603–2605.

27 (*a*) H. Bock and W. Helfrich, *Liq. Cryst.*, 1992, **12**, 697–703; (*b*) P. Henderson, H. Ringsdorf and P. Schuhmacher, *Liq. Cryst.*, 1995, **18**, 191–195; (*c*) S. Zamir, D. Singer, N. Spielberg, E. J. Wachtel, H. Zimmermann, R. Poupko and Z. Luz, *Liq. Cryst.*, 1996, **21**, 39–50.

28 (*a*) B. Alameddine, O. F. Aebischer, W. Amrein, B. Donnio, R. Deschenaux, D. Guillon, C. Savary, D. Scanu,

O. Scheidegger and T. A. Jenny, *Chem. Mater.*, 2005, **17**, 4798–4807; (*b*) M. Danz, R. Tonner and G. Hilt, *Chem. Commun.*, 2012, **48**, 377–379; (*c*) A. Pradhan, P. Dechambenoit, H. Bock and F. Durola, *Angew. Chem., Int. Ed.*, 2011, **50**, 12582–12585; (*d*) L. Dossel, L. Gherghel, X. Feng and K. Mullen, *Angew. Chem., Int. Ed.*, 2011, **50**, 2540–2543.

29 (*a*) S. Kumar and J. J. Naidu, *Liq. Cryst.*, 2001, **28**, 1435–1437; (*b*) S. Kumar, J. J. Naidu and D. S. Shankar Rao, *J. Mater. Chem.*, 2002, **12**, 1335–1341.

30 (*a*) J. He, D. M. Agra-Kooijman, G. Singh, C. Wang, C. Dugger, J. Zeng, L. Zang, S. Kumar and C. Scott Hartley, *J. Mater. Chem. C*, 2013, **1**, 5833–5836; (*b*) P. J. Repasky, D. M. Agra-Kooijman, S. Kumar and C. Scott Hartley, *J. Phys. Chem. B*, 2016, **120**, 2829–2837.

31 (*a*) Z. Li, N. T. Lucas, Z. Wang and D. Zhu, *J. Org. Chem.*, 2007, **72**, 3917–3920; (*b*) Z. Li, L. Zhi, N. T. Lucas and Z. Wang, *Tetrahedron*, 2009, **65**, 3417–3424; (*c*) D. Wu, H. Zhang, J. Liang, H. Ge, C. Chi, J. Wu, S. Liu and J. Yin, *J. Org. Chem.*, 2012, **77**, 11319–11324.

32 (*a*) K. Praefcke, A. Eckert and D. Blunk, *Liq. Cryst.*, 1997, **22**, 113–119; (*b*) N. Boden, R. J. Bushby, A. N. Cammidge, S. Duckworth and G. Headdock, *J. Mater. Chem.*, 1997, **7**, 601–605.

33 S. Zamir, R. Poupko, Z. Luz, J. B. Hiker, C. Boeffel and H. Zimmermann, *J. Am. Chem. Soc.*, 1994, **116**, 1973–1980.

34 G. W. Gray and J. W. Goodby, *Smectic Liquid Crystals. Textures and Structures*, Leonard Hill, Glasgow, 1984.

35 H. Hervet, F. Volino, A. J. Dianoux and R. E. Lechner, *Phys. Rev. Lett.*, 1975, **34**, 451–454.

36 (*a*) F. Lincker, B. Heinrich, R. De Bettignies, P. Rannou, J. Pécaut, B. Grévin, A. Pron, B. Donnio and R. Demadrille, *J. Mater. Chem.*, 2011, **21**, 5238–5247; (*b*) D. Zeng, I. Tahar-Djebbar, Y. Xiao, F. Kameche, N. Kayunkid, M. Brinkmann, D. Guillon, B. Heinrich, B. Donnio, D. A. Ivanov, E. Lacaze, D. Kreher, F. Mathevet and A.-J. Attias, *Macromolecules*, 2014, **47**, 1715–1731.

37 Y. Xiao, X. Su, L. Sosa-Vargas, E. Lacaze, B. Heinrich, B. Donnio, D. Kreher, F. Mathevet and A.-J. Attias, *CrystEngComm*, 2016, **18**, 4787–4798.

38 (*a*) D. Guillon and A. Skoulios, *Mol. Cryst. Liq. Cryst.*, 1983, **91**, 341–352; (*b*) A.-J. Attias, C. Cavalli, B. Donnio, D. Guillon, P. Happiot and J. Malthête, *Chem. Mater.*, 2002, **14**, 375–384.

39 A. C. Ribeiro, B. Heinrich, C. Cruz, H. T. Nguyen, S. Diele, M. W. Schröder and D. Guillon, *Eur. Phys. J. E: Soft Matter Biol. Phys.*, 2003, **10**, 143–151.

40 B. Alameddine, O. F. Aebischer, B. Heinrich, D. Guillon, B. Donnio and T. A. Jenny, *Supramol. Chem.*, 2014, **26**, 125–137.

41 H. Monobe, Y. Shimizu, S. Okamoto and H. Enomoto, *Mol. Cryst. Liq. Cryst.*, 2007, **476**, 31–41.

42 H. Iino, J. Hanna, R. J. Bushby, B. Movaghar and B. J. Whitaker, *J. Appl. Phys.*, 2006, **100**, 043716.

43 A. Ochse, A. Kettner, J. Kopitzke, J. H. Wendorff and H. Bassler, *Phys. Chem. Chem. Phys.*, 1999, **1**, 1757–1760.

44 R. J. Bushby and D. J. Tate, in *Liquid crystalline semiconductors*, ed. R. J. Bushby, S. M. Kelly and M. O'Neill, Springer, 2013.

45 R. J. Bushby, K. J. Donovan, T. Kreouzis and O. R. Lozman, *Opto-Electron. Rev.*, 2005, **13**, 269–279.

46 K.-Q. Zhao, X.-Y. Bai, B. Xiao, Y. Gao, P. Hu, B.-Q. Wang, Q.-D. Zeng, C. Wang, B. Heinrich and B. Donnio, *J. Mater. Chem. C*, 2015, **3**, 11735–11746.

47 K.-Q. Zhao, Y. Gao, W.-H. Yu, P. Hu, B.-Q. Wang, B. Heinrich and B. Donnio, *Eur. J. Org. Chem.*, 2016, 2802–2814.

